Dancing on the Saddles: A Geometric Framework for Stochastic Equilibrium Dynamics[†]

Hanbaek Lee[‡]

February 2026

(click here for the latest version)

Abstract

This paper extends deterministic saddle-path analysis to stochastic environments by introducing *conditional saddle paths*: the equilibrium path under frozen exogenous states. This concept yields a global geometric representation of stochastic equilibrium dynamics, in which equilibrium fluctuations decompose into movements *along* (endogenous propagation) and *across* (exogenous state transitions) conditional saddle paths. The framework delivers two theoretical results. First, state-dependent impulse responses arise from differences in the slopes of conditional saddle paths. Second, if an aggregate equilibrium variable varies strictly monotonically along conditional saddle paths, it uniquely indexes equilibrium states and thus provides an exact one-dimensional sufficient statistic. Applying this result, I prove that aggregate capital is a sufficient statistic in a canonical heterogeneous-household model (Krusell and Smith, 1998).

Keywords: Conditional saddle path, business cycles, state-dependent dynamics, sufficient statistics, heterogeneous agents.

JEL codes: C62, D58, E32.

[†]I am grateful for helpful comments and discussions from Timo Boppart, Francisco Buera, Vasco Carvalho, Minsu Chang, Rachel Childers, Elisa Giannone, Dirk Krueger, Benjamin Larin, Danial Lashkari, Tim Lee, Benjamin Moll, Tommaso Porzio, and Yucheng Yang. All errors are my own.

[‡]University of Cambridge. Email: hl610@cam.ac.uk

1 Introduction

Understanding equilibrium dynamics in models with aggregate uncertainty remains a central challenge in macroeconomics. Unlike deterministic models, where saddle-path diagrams provide immediate geometric intuition, stochastic equilibrium models lack comparable geometric frameworks. This makes it difficult to develop intuition about how economies respond to shocks, how different states interact, and why certain computational methods work. The challenge becomes particularly acute in heterogeneous-agent models, where the natural state variable is an infinite-dimensional wealth distribution—yet computational work routinely achieves dimension reduction to low-dimensional aggregates. Can we extend geometric saddle-path analysis to stochastic environments? What does such a framework reveal about equilibrium dynamics, state-dependent responses, and the success of computational approximations?

This paper makes two contributions. First, it extends the saddle-path analysis of equilibrium dynamics from deterministic models to stochastic environments by introducing the notion of *conditional saddle path*: equilibrium trajectories of the regime-frozen economy (holding the exogenous state fixed at a level). This geometric object decomposes business-cycle fluctuations into movements *along* a conditional saddle (endogenous propagation) and *across* conditional saddles (transitions when the exogenous state changes), providing a unified framework for analyzing state-dependent equilibrium dynamics. The framework enables visualization of generalized impulse responses and nonlinear transition dynamics in phase diagrams, analogous to how saddle-path diagrams illuminate deterministic models. Based on this geometric framework, I establish that state-dependent shock responses arise essentially from differences in the local slopes along the conditional saddle paths.

Second, it provides a general dimension-reduction theorem on the conditional saddle paths. If an aggregate equilibrium variable is strictly monotone and convergent along the conditional saddle, then it is injective on the invariant equilibrium set and hence uniquely indexes all equilibrium allocations and prices. As a consequence, the equilibrium can be represented *exactly*—not merely approximately—with a one-dimensional sufficient statistic. Applying this theoretical result, I establish that aggregate capital is a sufficient statistic for canonical heterogeneous-agent models (Krusell and Smith, 1998). To be precise, K-sufficiency means that the distributional state Φ is uniquely recoverable from K along the equilibrium path—not that K follows a sim-

ple (e.g., log-linear or Markovian) law of motion. The former is an exact theoretical result; the latter remains a quantitative approximation. This provides a geometric foundation for the practical success of scalar state approximations in business-cycle applications and delivers economically interpretable sufficient conditions for exact one-dimensional representations on the relevant invariant set.

These results extend beyond the canonical one-asset setting. In heterogeneous-agent models with multiple endogenous state variables, such as risky and riskless assets, liquid and illiquid assets, domestic and foreign bonds, the same logic applies (Krusell and Smith, 1997; Mendoza, 2010; Khan and Thomas, 2013; Kaplan and Violante, 2014; Berger and Vavra, 2015; Kaplan et al., 2018): whenever a monotone-convergent aggregate coordinate exists along conditional saddle paths, equilibrium dynamics remain exactly traceable by a scalar index.

Conditional saddle paths are equilibrium paths defined under frozen exogenous aggregate states: they describe counterfactual equilibrium continuations — how the economy would evolve if the aggregate state were held fixed at a given value — computed under the same decision rules that govern the stochastic equilibrium with regime switching. These counterfactual paths are economically meaningful because equilibrium decisions internalize the possibility of future regime changes, and the frozen-regime objects formalize the corresponding equilibrium "thought experiments."

Conditional saddle paths are closely connected to the random dynamical systems (RDS) notion of invariant manifolds for dynamics under exogenous forcing (Arnold, 1998; Schenk-Hoppé, 2001). In the present setting, the forcing is the aggregate Markov state, and a recursive competitive equilibrium (RCE) implies a time-homogeneous endogenous law of motion; conditional saddle paths are the discrete counterpart of the invariant manifolds from the frozen-regime equilibrium maps. Both perspectives organize stochastic dynamics using invariant geometric objects rather than local linearizations. The distinction in this paper is therefore not the mathematics of invariance, but the equilibrium discipline: the invariant-manifold structure is pinned down by optimality, market clearing, and equilibrium consistency, and it is precisely what makes global transition functions and impulse responses well defined and comparable across aggregate states within the recursive equilibrium framework.

The framework applies to any recursive competitive equilibrium with a predetermined endogenous state. In addition to the RBC and heterogeneous-agent applications developed here, companion work applies conditional saddle paths to New

Keynesian models with an occasionally binding zero lower bound (Lee and Nomura, 2026), where the kink in the conditional saddle at $i_{-1} = 0$ provides a geometric characterization of the ZLB's effect on equilibrium dynamics, and to production network economies with endogenous linkage formation (Lee and Sun, 2026), where a sign reversal in the conditional saddle slopes across regimes generates duration-dependent business cycle asymmetry. Section 4.3 illustrates the framework in a search-and-matching environment.

Related literature This paper contributes to three strands of literature in macroeconomics. The first is the literature studying global equilibrium dynamics and solution methods under aggregate uncertainty. The challenge of characterizing equilibrium dynamics in models with aggregate shocks has motivated extensive methodological development. Marcet (1988), Den Haan and Marcet (1990) and Krusell and Smith (1998) pioneered the use of bounded rationality approximations. In particular, Krusell and Smith (1998) discovered that a simple linear forecasting rule in aggregate capital achieves remarkable accuracy ($R^2 > 0.9999$) despite the infinite-dimensional state space. Thereafter, the literature has dramatically developed to sharpen the accuracy and improve the computational efficiency by incorporating moment-based approximations, exact aggregation, functional approximations, sequence-space approaches, and machine/deep learning (Den Haan, 1996, 1997; Reiter, 2001; Algan et al., 2008, 2010; Den Haan and Rendahl, 2010; Reiter, 2010; Ahn et al., 2018; Boppart et al., 2018; Elenev et al., 2021; Auclert et al., 2021; Cao et al., 2023; Azinovic et al., 2022; Fernández-Villaverde et al., 2023; Han et al., 2025; Payne et al., 2025).

This paper differs from these computational contributions by providing geometric foundations for *why* dimension reduction works. Rather than developing new algorithms, I introduce conditional saddle paths as a geometric framework for understanding equilibrium dynamics — analogous to how saddle-path diagrams provide intuition in deterministic models. The framework reveals that aggregate capital's sufficiency in a canonical heterogeneous-household model follows from geometric properties (nullcline invariance and monotonicity) rather than numerical happenstance.

The exact sufficiency result also has computational implications. Lee (2025) develops a repeated transition method that constructs conditional expectations for individual-level problems by identifying periods in simulations, where aggregate states are similar, enabling reuse of computed transitions across these similar states. The

method requires a metric for determining when aggregate states are "close enough" to pool. My sufficiency result establishes that aggregate capital distance provides a theoretically justified metric — agents' problems are identical whenever capital stocks coincide, regardless of distributional differences. This validates distance-based pooling strategies and enables efficient implementation without requiring explicit distributional tracking.[1]

This paper builds on the traditional use of geometric methods to analyze economic dynamics in deterministic environments. Phase-diagram analyses of the Solow–Swan (Solow, 1956; Swan, 1956) and Ramsey–Cass–Koopmans (Ramsey, 1928; Cass, 1965; Koopmans, 1963) growth models provide foundational intuition about convergence and stability. I extend this geometric approach to stochastic environments by introducing conditional saddle paths. This framework offers a geometric interpretation of stochastic equilibrium dynamics, including nonlinear and state-dependent impulse responses. In particular, it provides a useful visual tool for understanding how microfounded frictions generate state-dependent dynamics, as documented in the recent literature (Kaplan and Violante, 2014; Vavra, 2014; Berger and Vavra, 2015; Basu and Bundick, 2017; Bloom et al., 2018; Kaplan et al., 2018; Petrosky-Nadeau et al., 2018; Baley and Blanco, 2019; Pizzinelli et al., 2020; Berger et al., 2021; Melcangi, 2024; Winberry, 2021; Lee, 2026).

Finally, in mathematics, the literature on random dynamical systems provides foundational tools for geometric analyses of stochastic dynamic processes. However, its focus has not been on history-invariant saddle paths of the type that arise in recursive competitive equilibrium (Arnold, 1998; Schenk-Hoppé, 1998; Schenk-Hoppé, 2001).[2] For example, Yannacopoulos (2011) introduces the notion of stochastic saddle paths, which are conceptually distinct from conditional saddle paths in that they vary with the realized history of shocks.[3]

[1] The idea of solving heterogeneous-agent models by freezing the aggregate state and analyzing transitions appears in several computational approaches, including Bourany (2018), Section 4.3 of a working paper version of Achdou et al. (2021), and Lee (2025). The present paper provides a theoretical foundation: conditional saddle paths formalize the underlying geometric objects, and the sufficiency results explain when dimension reduction is exact.

[2] In the language of Random Dynamical Systems, the conditional steady state corresponds to a deterministic realization of the random fixed point (Schenk-Hoppé and Schmalfuß, 2001), while the conditional saddle path represents the invariant manifold of the frozen-regime dynamics (Arnold, 1998).

[3] Stochastic saddle paths depend on the specific sequence of past realizations, whereas conditional saddle paths are invariant to history.

By contrast, conditional saddle paths furnish economists with a geometric representation of stochastic equilibrium dynamics that is directly analogous to the role of phase diagrams in deterministic models. While this framework relies on standard regularity conditions to ensure well-defined and bounded equilibrium paths (Kamihigashi, 2003, 2005), the emphasis here is not on establishing existence results, but rather on providing geometric tools for understanding and analyzing stochastic equilibrium dynamics.

2 Conditional saddle path

2.1 Definitions and assumptions

I consider a generic dynamic stochastic model where the corresponding recursive competitive equilibrium (RCE) is characterized by the following aggregate state S and the endogenous and exogenous law of motions $(\Gamma_{endo}, \Gamma_{exo})$:

$$S = [\Phi, A] \tag{1}$$

where Φ is the endogenous aggregate state variable, and A is the exogenous aggregate state variable. The latter admits a multivariate vector that follows a stochastic process. I assume the exogenous aggregate law of motion Γ_{exo} is a Markov chain. For simplicity in the illustration, I assume Γ_{exo} is a two-state Markov chain where $A \in \{B, G\}$, and $\Gamma_{exo}(A'|A) > 0$ for $\forall A', A$.

I consider a distributional state space $\mathcal{X}$, whose elements $\Phi \in \mathcal{X}$ summarize the cross-sectional distribution of idiosyncratic household states that are payoff-relevant for equilibrium (e.g., assets and employment/productivity types) together with any endogenous objects needed to evaluate equilibrium decision rules. Formally, one can take $\mathcal{X}$ to be a subset of a metric space of probability measures augmented, if needed, by a finite-dimensional vector of aggregate variables. Throughout, $\Gamma_{\text{endo}}(\cdot, A) : \mathcal{X} \to \mathcal{X}$ denotes the recursive equilibrium law of motion mapping the current distributional state into the next-period state under frozen regime A.

Definition 1 (Conditional saddle path)**.**
Fix a regime $A \in \{B, G\}$ and an initial state $\Phi_0 \in \mathcal{X}$. Let $\{\Phi_t\}_{t\geq 0}$ denote the frozen-

regime continuation under A, defined recursively by

$$\Phi_{t+1} = \Gamma_{\text{endo}}(\Phi_t, A), \qquad t \geq 0. \tag{2}$$

The conditional saddle path under A from Φ_0 is defined as the closure of the frozen-regime continuation:

$$\mathcal{M}(\Phi_0, A) := \overline{\{\Phi_t : t \geq 0\}}. \tag{3}$$

Throughout, the distributional state space is a metric space of probability measures $(\mathcal{X}, d)$, where d is compatible with weak convergence of distributions. The closure in Definition 1 is taken with respect to this metric. The frozen-regime continuation $\{\Phi_t\}_{t\geq 0}$ is a sequence in $\mathcal{X}$, and $\mathcal{M}(\Phi_0, A) := \overline{\{\Phi_t : t \geq 0\}}$ is its closure in $(\mathcal{X}, d)$. Based on the conditional saddle path, conditional steady state is defined as follows:

Definition 2 (Conditional steady state)**.**
Given (Φ_0, A_0), if the frozen-regime continuation $\{\Phi_t\}_{t\geq 0}$ converges, I denote its limit by

$$\Phi^{cs}(\Phi_0, A) \;:=\; \lim_{t\to\infty} \Phi_t. \tag{4}$$

Definition 1 defines the conditional saddle path directly from the frozen-regime continuation. Fixing A makes the equilibrium law of motion deterministic on the distribution space: starting from Φ_0, the sequence $\{\Phi_t\}_{t\geq 0}$ is generated by repeated application of the endogenous transition operator $\Gamma_{\text{endo}}(\cdot, A)$. In this sense, $\mathcal{M}(\Phi_0, A)$ is the natural analogue of the saddle arm in deterministic saddle-path analysis: it isolates the equilibrium states visited (and their limit points) along the economically relevant convergence dynamics under regime A.[4]

Assumption 1 (Regularity of conditional saddle paths)**.**
Fix a regime $A \in \{B, G\}$ and an initial state $\Phi_0 \in \mathcal{X}$. Let $\{\Phi_t\}_{t\geq 0}$ be defined by

[4]Strictly speaking, $\mathcal{M}(\Phi_0, A) = \overline{\{\Phi_t : t \geq 0\}}$ as defined in discrete time is an orbit-closure (a countable set together with its limit point) and therefore need not be a smooth manifold. I nonetheless use saddle-path language to emphasize its one-dimensional, path-like role for global dynamics. In a continuous-time formulation with a smooth flow on the state space, the corresponding stable branch is naturally represented as a one-dimensional invariant manifold under standard regularity conditions.

$\Phi_{t+1} = \Gamma_{\text{endo}}(\Phi_t, A)$.

(i) (Unique existence) The conditional steady state $\Phi^{cs}(\Phi_0, A)$ *uniquely exists on* $\mathcal{M}(\Phi_0, A)$.

(ii) (Continuity) The map $\Gamma_{\text{endo}}(\cdot, A) : \mathcal{X} \to \mathcal{X}$ *is continuous. Moreover, the aggregate variables (e.g., aggregate capital* K *and consumption* C*) vary continuously in* Φ *when restricted to* $\mathcal{M}(\Phi_0, A)$.

Assumption 1 collects the regularity properties of the conditional saddle path that are needed for the paper's geometric arguments. Assumption 1 (i) assumes that, conditional on a regime A and an initial state Φ_0, the frozen-regime continuation converges to a unique conditional steady state within the relevant invariant equilibrium set. This does not assert global uniqueness across all initial conditions, which would require stronger fixed-point arguments, nor does it rule out multiplicity across initial conditions or regimes.

In particular, Proehl (2025) establishes global existence and uniqueness of recursive equilibrium in heterogeneous-agent models under parametric restrictions, whereas Assumption 1 (i) allows for the possibility of global multiplicity as in Walsh and Young (2024).[5] A full characterization of primitives ensuring Assumption 1 (i) is beyond the scope of this paper.

Assumption 1 (ii) imposes continuity of the frozen-regime law of motion and of the relevant aggregate observables when restricted to the conditional saddle. This mild regularity ensures that small perturbations of the distributional state *within the equilibrium set under study* produce small changes in aggregate outcomes and subsequent states, which is used repeatedly when translating geometric properties of projected phase diagrams (e.g., nullclines) into restrictions on equilibrium dynamics along the saddle.

With this geometric regularity in place, the conditional saddle admits a natural notion of "position along the curve" toward the conditional steady state. Theorem 2 formalizes the key implication: if some aggregate equilibrium variable moves strictly one-way along this curve, then it provides a valid coordinate for the entire conditional saddle. In that case, knowing the scalar value is equivalent to knowing the full

[5]Nevertheless, conditional on a given initial state and a fixed regime, the equilibrium path considered in the analysis is assumed to be uniquely determined.

distributional state within the relevant equilibrium set, so the stochastic equilibrium admits an exact one-dimensional representation on $\mathcal{M}(\Phi_0, A)$.

2.2 Representative-agent economy: A canonical RBC

A representative household with temporal log utility is considered. Given initial condition (a_0, A_0), the household maximizes life-time utility under stochastic aggregate TFP A_t. I present the economy in recursive form and work with a recursive competitive equilibrium. Under standard regularity conditions (including an appropriate transversality condition), this recursive formulation is equivalent to the sequential equilibrium; for completeness the sequential formulation is provided in Appendix A. The recursive form of the household's problem is as follows:

$$v(a; K, A) = \max_{c, a'} \quad log(c) + \beta \mathbb{E} v(a'; K', A') \tag{5}$$

$$c + a' = a(1 + r(X)) + w(X) \tag{6}$$

$$a' \geq -\overline{a} \tag{7}$$

$$K' = \Gamma_{endo}(K, A), \quad A' \sim \Gamma_{exo}(A'|A), \tag{8}$$

where v is the household's value function; a is the wealth in the beginning of a period; K is aggregate capital; A is aggregate TFP; Γ_{endo} is the law of motion for K. For illustrative purposes, I assume that TFP A follows a Markov-switching process between the levels B and G, where $G > B$:

$$\Gamma_{exo} = \begin{bmatrix} \pi_{BB} & \pi_{BG} \\ \pi_{GB} & \pi_{GG} \end{bmatrix} \tag{9}$$

I consider the following competitive factor prices given CRS Cobb-Douglas production function:

$$r(K, A) = A\alpha K^{\alpha - 1} - \delta \tag{10}$$

$$w(K, A) = A(1 - \alpha) K^{\alpha}, \tag{11}$$

where K is capital stock, which satisfies $K = a$ in equilibrium. The recursive competitive equilibrium (RCE, hereafter) is as follows:

Definition 3 (Recursive competitive equilibrium)**.**
$(c, a', v, r, w, \Gamma_{endo})$ *is a recursive competitive equilibrium if these functions*

1. *satisfy the individual optimality conditions*
2. *clear factor markets, resulting in the competitive prices.*
3. *satisfy the consistency:*

$$a'(K; K, A) = K' = \Gamma_{endo}(K, A) \tag{12}$$

Based on the endogenous law of motion Γ_{endo} defined in the recursive competitive equilibrium of Definition 3, I define conditional K-nullcline.

Definition 4 (Conditional K-nullcline in RBC)**.**
Fix (K_0, A_0) *and a regime* $A \in \{B, G\}$*. Let* $\{K_t\}_{t\geq 0}$ *be the frozen-regime continuation* $K_{t+1} = \Gamma_{\text{endo}}(K_t, A)$*. The conditional* K*-nullcline along the continuation is*

$$\mathcal{N}(A; K_0) := \Big\{(K_t, C_t) : \ t \geq 0, K_{t+1} - K_t = 0\Big\}, \ C_t := C(K_t, A) \tag{13}$$

where C *is the aggregate equilibrium consumption variable. When* $\mathcal{N}(A; K_0)$ *is the graph of a function, define* $C_A^{Kcnull}(\cdot; K_0)$ *by* $\mathcal{N}(A; K_0) = \{(K, C) : \ C = C_A^{Kcnull}(K; K_0)\}$*.*

Then, in the simple RBC model, we can explicitly characterize the conditional K-nullcline. In particular, the nullcline is independent of the initial condition K_0.

Proposition 1 (Characterizing the conditional K-nullcline in RBC)**.**
The conditional nullclines of aggregate capital K *for* $A \in \{B, G\}$ *are as follows:*

$$C_A^{Kcnull}(K) = AK^{\alpha} - \delta K, \tag{14}$$

thus, $C_A^{Kcnull}(K)$ *is independent of* K_0*.*

Proof. From the stationary condition for the capital stock ($\delta K = I$) and the national accounting identity ($Y = C + I$), the conditional nullclines of aggregate capital K for $A \in \{B, G\}$ are as $C_A^{Kcnull}(K) = AK^{\alpha} - \delta K$. ■

In optimal dynamics, the conditional saddle path can exhibit discrete-time pathologies in which the projected (K, C) trajectory develops folds or loops. In such cases the

saddle may (i) touch the K-nullcline at an intermediate point $K \neq K_A^{cs}$ (a "turning point") or (ii) alternate sides of the nullcline across dates (a "spiral"). To rule out these pathologies, I impose the following geometric restriction on one-step transitions in the (K, C) plane.

Assumption 2 (No segment crossing of the conditional K-nullcline)**.**
A straight line segment in (K, C) connecting (K_t, C_t) and (K_{t+1}, C_{t+1}) does not intersect the conditional K-nullcline for $\forall A \in \{B, G\}$:

$$[(K_t, C_t), (K_{t+1}, C_{t+1})] \cap \mathcal{N}(A) = \emptyset, \ \forall t \geq 0. \tag{15}$$

Assumption 2 is a discrete-time "no side-switching" condition: along the frozen-regime continuation, consecutive points (K_t, C_t) and (K_{t+1}, C_{t+1}) remain in the same region of (K, C)-space separated by the K-nullcline. In particular, letting $H_t := C_t - C_A^{Kcnull}(K_t)$, Assumption 2 implies $H_t H_{t+1} > 0$ for all t prior to convergence, so net investment $\Delta K_t := K_{t+1} - K_t = C_A^{Kcnull}(K_t) - C_t = -H_t$ cannot reverse sign along the conditional saddle.

In continuous time, reversals of $\dot{K}$ necessarily pass through $\dot{K} = 0$, so continuity of the drift often delivers a comparable one-crossing geometry along the stable branch in standard settings. In discrete time, by contrast, the time-t map can jump across the nullcline between dates without ever landing on it at an integer time. Assumption 2 rules out such nonlocal crossings and thereby ensures a well-behaved saddle geometry consistent with reporting global impulse responses and transition functions as single-valued equilibrium objects.[6]

Section 4.1 provides primitive sufficient conditions under which Assumption 2 holds in the heterogeneous-household economy (Krusell and Smith, 1998). The argument leverages bounds on households' marginal propensities to consume out of price-induced changes in contemporaneous income and shows that sufficiently weak general-equilibrium price feedback rules out discrete-time side-switching across the K-nullcline.

Proposition 2 (K monotonicity in RBC)**.**

[6]Discrete time admits nonlocal movements that can generate folds or repeated nullcline intersections in the projected (K, C) dynamics even when the underlying saddle is one-dimensional. Assumption 2 rules out such pathologies along the conditional saddle. For related geometric restrictions in dynamic optimization, see Reddy et al. (2020) and, on threshold (Skiba) phenomena, Skiba (1978), Dechert and Nishimura (1983), and Wagener (2003).

Fix $A \in \{B, G\}$. Under Assumptions 1 and 2, aggregate capital along the frozen-regime continuation converges to K_A^{cs} strictly monotonically.

Proof. Fix A and let $\{\Phi_t\}_{t\geq 0}$ be the frozen-regime continuation, with $K_t := K(\Phi_t)$ and $C_t := C(\Phi_t, A)$. Define net investment

$$\Delta K_t := K_{t+1} - K_t. \tag{16}$$

In the RBC benchmark, the aggregate resource constraint implies the K-nullcline representation

$$\Delta K_t = C_A^{Kcnull}(K_t) - C_t, \tag{17}$$

so the sign of ΔK_t is the opposite of the nullcline gap $H_t := C_t - C_A^{Kcnull}(K_t)$.

By Assumption 2, for every t such that $\Phi_t \neq \Phi^{cs}(\Phi_0, A)$, the segment connecting (K_t, C_t) and (K_{t+1}, C_{t+1}) does not intersect the K-nullcline. Since the K-nullcline is the graph of a continuous function, this implies $H_t H_{t+1} > 0$, hence $\{H_t\}$ has a constant sign prior to convergence. Therefore $\Delta K_t = -H_t$ has a constant nonzero sign whenever $\Phi_t \neq \Phi^{cs}(\Phi_0, A)$, and $\{K_t\}$ is strictly monotone in t until convergence.

Finally, Assumption 1 (i) implies $\Phi_t \to \Phi^{cs}(\Phi_0, A)$, and continuity of K (Assumption 1 (ii)) yields $K_t \to K_A^{cs} := K(\Phi^{cs}(\Phi_0, A))$. ■

In the model, the household ex-ante takes into account the aggregate uncertainty in its decision. The conditional saddle path is the sequence of outcomes implied by such ex-ante decisions when the ex-post exogenous aggregate states are *frozen* at A. Figure 1 depicts the conditional saddle paths of the calibrated RBC model in the (K, C) plane under the two aggregate productivity regimes $A \in \{B, G\}$. The model is solved globally using the repeated transition method of Lee (2025) under the standard quarterly calibration. For each regime A, I construct the frozen-regime continuation by holding productivity fixed at A for 2,000 periods and iterating the equilibrium law of motion from two initial capital stocks: one sufficiently low to generate the upward-converging branch and one sufficiently high to generate the downward-converging branch.[7]

[7] This procedure traces the stable branch from both sides of the conditional steady state and is used only to recover the full conditional saddle in the phase diagram; the equilibrium continuation itself is single-valued given (Φ_0, A).

Panel (a) provides a zoom-in around the conditional steady states and reports a histogram of simulated (K_t, C_t) outcomes under the stochastic regime-switching economy, showing that realized dynamics concentrate near and move along the relevant saddle geometry. Panel (b) zooms out to emphasize the global partition of the (K, C) plane and the associated direction of net-investment dynamics under each regime. In panel (b), the conditional K-nullclines (labeled $\Delta K|_A = 0$) are overlaid; in the RBC benchmark they are sign-determining via $\Delta K = C_A^{Kcnull}(K) - C$. Direction arrows indicate the frozen-regime evolution along each conditional saddle.

The global dynamics of the recursive competitive equilibrium are fully characterized by movements along and across these conditional saddle paths. When aggregate productivity remains constant, the economy evolves along the corresponding saddle path. If the economy is initialized between the two conditional saddle paths and $A = G$, capital converges strictly monotonically upward toward the conditional steady state K_G^{cs}; if $A = B$, capital converges strictly monotonically downward toward K_B^{cs} consistent with Proposition 2. If the initial state lies outside this region, the economy gradually transitions into it while moving along the relevant saddle paths.

MIT shock on the saddle This decomposition of the dynamics yields a sharp characterization of unexpected transitory shocks (MIT shocks). Any MIT shock (whether TFP, monetary policy, fiscal, or any other unanticipated disturbance — including those not explicitly modeled) is necessarily mapped into a displacement along a conditional saddle path: there exists a magnitude of shift along the conditional saddle that is equivalent to the shock's impact, and all subsequent dynamics are along-path convergence. Consequently, the slope and curvature of the conditional saddle at the point of displacement fully determine the economy's propagation of the shock, including its persistence, amplification, and state dependence.

Along the conditional saddle, the economy evolves according to the law of motion Γ_{endo} for the endogenous state. In particular, the aggregate capital K strictly monotonically converges to the conditional steady state — if K is lower than a conditional steady state of the conditional saddle the economy is in, it increases, and vice versa for the case of K higher than it. This strictly monotonically converging pre-determined variable is the key to link the heterogeneous-agent model and the representative-agent model as in the current setup — the variable becomes the sufficient statistic for the heterogeneous-agent model.

Figure 1: Conditional saddle paths and the phase diagram

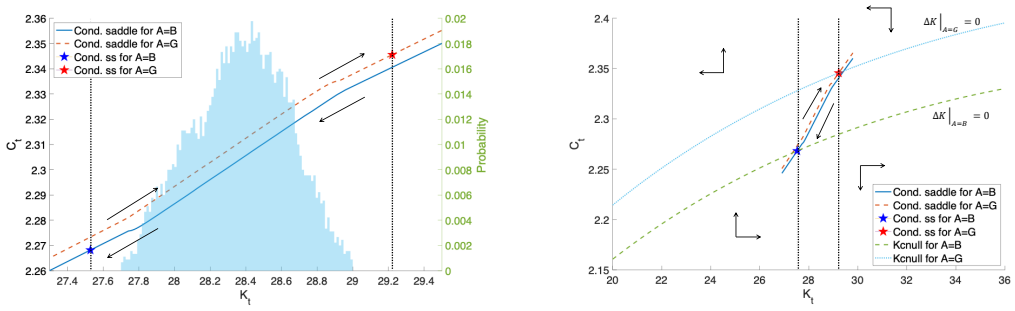

(a) Zoom-in (b) Zoom-out

Notes: The conditional K-nullclines (labeled $\Delta K = 0$) partition the (K, C) plane via $\Delta K = C_A^{Kcnull}(K) - C$. Direction arrows show the frozen-regime continuation along each conditional saddle. Panel (a) zooms into the neighborhood of the conditional steady states shown in panel (b). In panel (a), direction arrows indicate the frozen-regime evolution along each conditional saddle. The histogram in the background plots the time-series distribution of the aggregate capital stock. In panel (b), additional direction arrows are included to indicate the the global sign partition in the dynamics.

When the level of TFP exogenously changes, the economy jumps from one saddle to the other vertically – capital responds from the following period as it is a predetermined variable one period ahead. In this dynamics, the key force to move the economy is the law of motion for the exogenous state Γ_{exo}. Combined together, both law of motions generate bounded stochastic fluctuations in the economy.

Generalized transition function The conditional saddle path captures the entire transitions across different endogenous (along the saddle) and exogenous states (across the saddle), allowing generalized transition function (GTF) analysis (Lee, 2025), which encompasses generalized impulse response functions (Koop et al., 1996; Andreasen et al., 2017). The economy's response to a sequence of exogenous shocks is not confined to local dynamics around the steady state, and its trajectory is sharply traced in the phase diagram.

Figure 2 illustrates the equilibrium dynamics in consumption and capital stock in phase diagram (panel (a)) and in time domain (panels (b) and (c)) for an arbitrary subsample period (830 – 849, 20 quarters) in the equilibrium path. In period 830, an exogenous negative TFP shock hits leading to a downward jump in consumption across the conditional saddle paths. Then, for four consecutive periods, consumption and capital stock endogenously decline along the saddle. In period 835, an exogenous

positive TFP shock hits, shifting the economy to the other conditional saddle path, followed by upward endogenous adjustments in consumption and capital. Compared

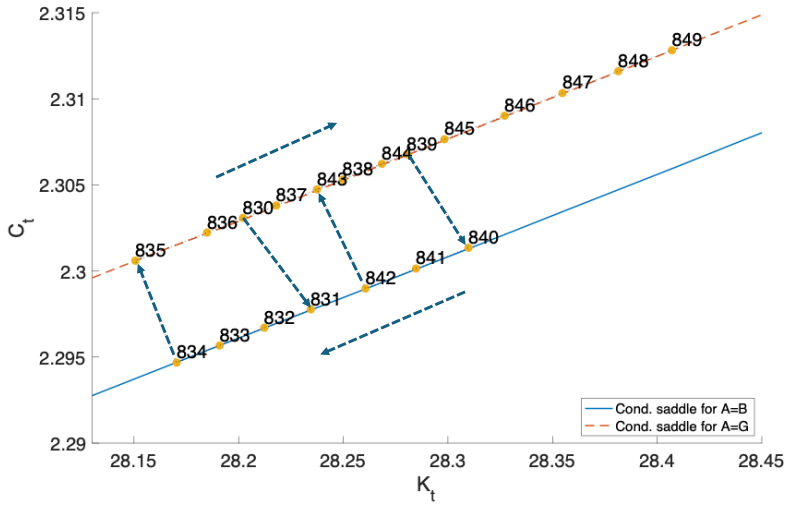

(a) On the saddles

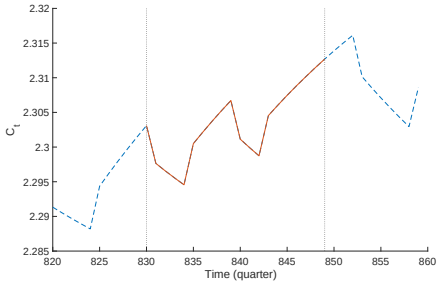

(b) C - time domain

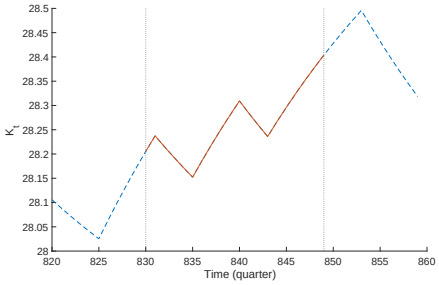

(c) K - time domain

Figure 2: Equilibrium dynamics: saddle vs. time domain

Notes: The figure illustrates the stochastic equilibrium dynamics of consumption and capital stock on the conditional saddle paths (panel (a)) and in the time domain (panels (b) and (c)) implied by a canonical RBC model under standard quarterly calibration. The sample period covers 20 quarters from 830 to 849.

to time-domain figures, the phase diagram more concisely illustrates the economy's equilibrium dynamics in a single figure. Moreover, it enables immediate consideration of counterfactual scenarios by eyeballing the realized exogenous paths.

As the information on all possible global equilibrium dynamics are contained in the conditional saddle paths, generalized impulse response function (GIRF) can be also conveniently represented. For the GIRF illustration I replace the two-state Markov chain with a continuous AR(1) process for A: $A' = (1-\rho)\mu + \rho A + \epsilon$, $\epsilon \sim N(0, \sigma)$. In

this case, there is a continuum of frozen-A conditional saddles indexed by A, and the GIRF path moves both along a given conditional saddle (endogenous propagation) and across the foliation as A evolves.

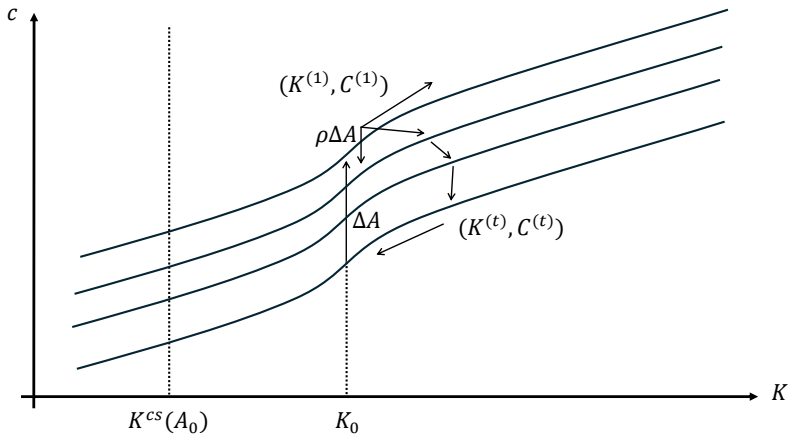

Figure 3: Generalized impulse response function (GIRF) at (K_0, A_0)

Notes: The figure illustrates the generalized impulse responses of consumption and capital stock on the conditional saddle paths to a positive TFP shock.

Figure 3 illustrates the post-shock dynamics in the phase diagram following a positive TFP shock, as aggregate productivity gradually reverts to its steady-state level. Upon impact, consumption jumps upward, inducing a vertical shift of the economy across conditional saddle paths. In subsequent periods, forces operating both along and across these saddles jointly shape the post-shock dynamics, generating a right-bending, bow-shaped trajectory. Consequently, the capital stock K exhibits an inverted-U-shaped impulse response over time, while consumption c displays a downward-sloping response in the time domain.

Figure 4 presents the simulated impulse responses of consumption and capital following a positive TFP shock, shown in the phase diagram (panel (a)) and in the time domain (panels (b) and (c)) over periods 1–50. Consistent with the phase-diagram intuition, the bow-shaped capital trajectory translates into a hump-shaped impulse response in the time domain, as shown in panel (c). Consumption also exhibits a hump-shaped response: initially, high-TFP conditional saddle paths push consumption upward, but as TFP gradually decays and crosses a threshold level, the direction of adjustment reverses, pulling consumption back down.

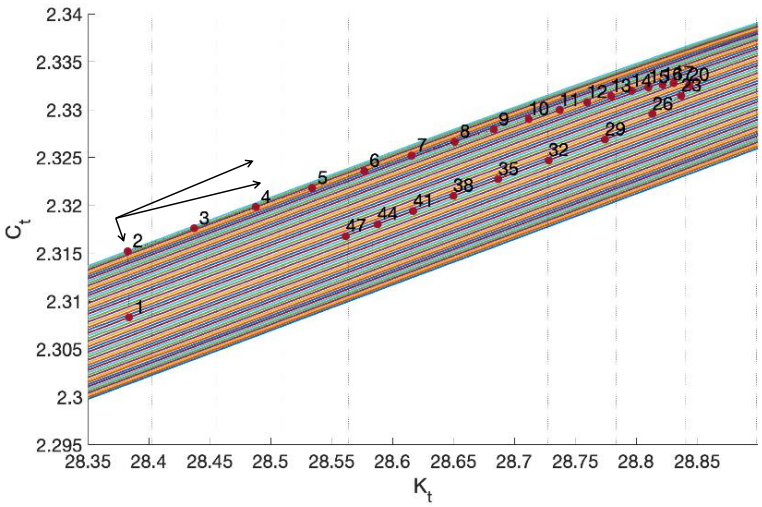

(a) On the saddles

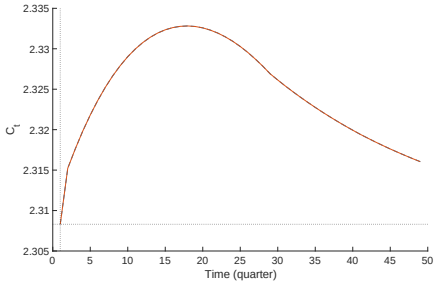

(b) C - time domain

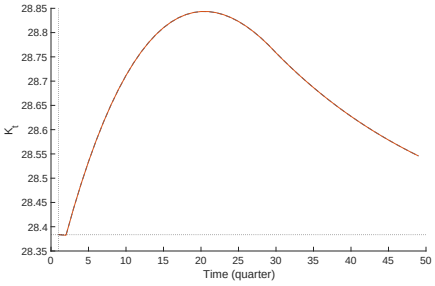

(c) K - time domain

Figure 4: Impulse responses to a positive TFP shock: saddle vs. time domain

Notes: The figure illustrates the impulse responses of consumption and capital stock on the conditional saddle paths (panel (a)) and in the time domain (panels (b) and (c)). The sample period covers 50 quarters from 1 to 50.

Comparison with the perfect-foresight saddles The household's inter-temporal optimality conditions evaluated at the conditional steady states are as follows:

$$\beta\pi_{BB}\overbrace{\left(1+\alpha B(K_B^{cs})^{\alpha-1}-\delta\right)}^{\text{Discounted return for } B\to B}+\beta\pi_{BG}\overbrace{\left(\frac{c(K_B^{cs},G)}{c_B^{cs}}\right)^{-1}\left(1+\alpha G(K_B^{cs})^{\alpha-1}-\delta\right)}^{\text{Discounted return for } B\to G}=1 \quad (18)$$

$$\beta\pi_{GG}\underbrace{\left(1+\alpha G(K_G^{cs})^{\alpha-1}-\delta\right)}_{\text{Discounted return for } G\to G}+\beta\pi_{GB}\underbrace{\left(\frac{c(K_G^{cs},B)}{c_G^{cs}}\right)^{-1}\left(1+\alpha B(K_G^{cs})^{\alpha-1}-\delta\right)}_{\text{Discounted return for } G\to B}=1 \quad (19)$$

These equations pin down the conditional steady-state conditions for the aggregate capital stocks K_B^{cs} and K_G^{cs}:

$$K_B^{cs} = \left(\frac{\alpha(\pi_{BB}B + \pi_{BG}G)}{1/\beta - (1-\delta)\left(\pi_{BB} + \pi_{BG}\left(g_c^{cs}(B)\right)^{-1}\right)} \right)^{\frac{1}{1-\alpha}} \tag{20}$$

$$K_G^{cs} = \left(\frac{\alpha(\pi_{GG}G + \pi_{GB}B)}{1/\beta - (1-\delta)\left(\pi_{GG} + \pi_{GB}\left(g_c^{cs}(G)\right)^{-1}\right)} \right)^{\frac{1}{1-\alpha}} \tag{21}$$

where $g_c^{cs}(A)$, $A \in \{B, G\}$ are gross consumption growth rates when a regime change happens in each conditional steady state.

In the *perfect-foresight (PF)* economy, agents believe regime switching is impossible and, consistent with this belief, the regime does not switch. In contrast, along the *conditional-saddle (CS)* dynamics, the regime is held fixed ex post, but agents still correctly anticipate that regime switches are possible under Π. Thus PF and CS share the same feasibility accounting and the same K-nullcline under a given productivity level, yet generally differ in their Euler-implied consumption dynamics and hence in their steady states and saddle paths.

Then, I consider a perfect-foresight dynamics where there is no uncertainty in the economy and TFP A is fixed at either B or G. I denote allocations for this perfect-foresight economy with superscript pf. Following a canonical neoclassical growth model analysis, I derive the steady states for the perfect-foresight counterpart with different TFP levels:

$$(K_B^{pf}, c_B^{pf}) = \left(\left(\frac{\alpha B}{1/\beta + \delta - 1} \right)^{\frac{1}{1-\alpha}}, B\left(\frac{\alpha B}{1/\beta + \delta - 1} \right)^{\frac{\alpha}{1-\alpha}} - \delta \left(\frac{\alpha B}{1/\beta + \delta - 1} \right)^{\frac{1}{1-\alpha}} \right) \tag{22}$$

$$(K_G^{pf}, c_G^{pf}) = \left(\left(\frac{\alpha G}{1/\beta + \delta - 1} \right)^{\frac{1}{1-\alpha}}, G\left(\frac{\alpha G}{1/\beta + \delta - 1} \right)^{\frac{\alpha}{1-\alpha}} - \delta \left(\frac{\alpha G}{1/\beta + \delta - 1} \right)^{\frac{1}{1-\alpha}} \right) \tag{23}$$

Notably, two economies share the same capital (conditional) nullclines for each productivity levels, as formalized in Proposition 3.

Proposition 3 (K-nullcline invariance over beliefs)**.**
Conditional K-nullclines are identical between the RBC model with the aggregate uncertainty and the perfect foresight counterpart.

Proof.

From the stationary condition $\delta K = I$, equation (14) are immediate for both models. Therefore, the conditional nullclines are the same. ■

This property provides two important insights. First, the differences in the limit behaviors of two economies (steady states) and the corresponding saddle paths are crucially determined by the consumption dynamics – consumption nullclines.[8] In Proposition 4, I compare the rankings between the baseline model and the perfect-foresight model.

Second, both with and without aggregate uncertainty, the saddle-path dynamics require the capital stock K to converge strictly monotonically to the (conditional) steady state. Even when the baseline model is extended to a heterogeneous-household environment, as in Section 4, the K-nullcline remains invariant, preserving the monotonicity of K along conditional saddle paths. This property is crucial for establishing the sufficiency of K in summarizing aggregate fluctuations in the heterogeneous-household setting.

Proposition 4 (Aggregate uncertainty and the conditional steady states)**.**
The following inequalities hold:

$$K_B^{cs} < K_B^{pf} < K_G^{pf} < K_G^{cs}, \qquad c_B^{cs} < c_B^{pf} < c_G^{pf} < c_G^{cs}. \tag{24}$$

Proof.
See Appendix C. ■

Proposition 4 shows that the (conditional) steady state associated with low TFP features lower capital stock and consumption under the aggregate uncertainty than under perfect foresight; the one with high TFP features the opposite. Therefore, conditional steady states of capital and consumption with perfect foresight are nested by the counterparts in the steady state with aggregate uncertainty. These are fully driven by rational expectations for future regime shifting under aggregate uncertainty.

Figure 5 plots the conditional saddle paths for the model with aggregate uncertainty and the perfect-foresight deterministic saddle paths. As shown in Proposition 4, conditional steady states for both capital stocks and consumption with perfect foresight are nested by the ones with aggregate uncertainty.

[8] Rigorously speaking, there is no consumption nullcline in the model with aggregate uncertainty. The Euler equations at the conditional steady states play the same role as the consumption nullclines without uncertainty.

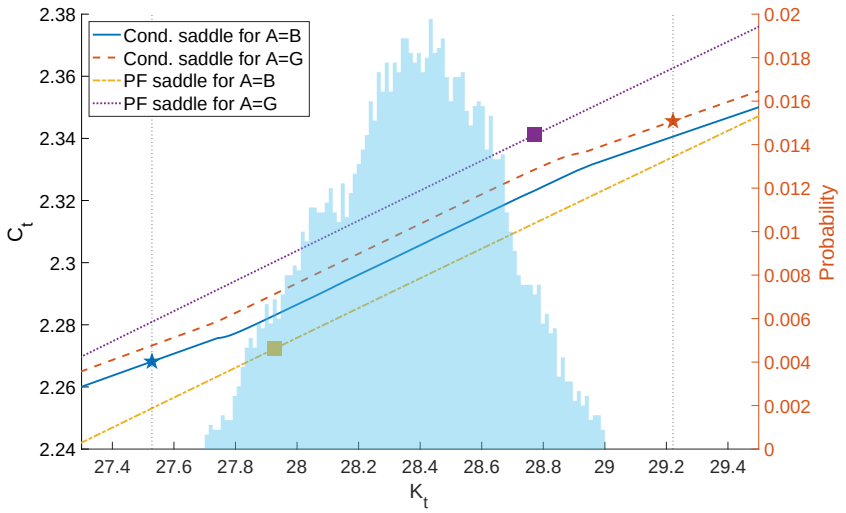

Figure 5: Conditional saddle path comparison: with and without uncertainty

Notes: The figure plots conditional saddle paths for $A = B$ (solid) and $A = G$ (dashed) and perfect-foresight saddle paths for $A = B$ (dash-dotted) and $A = G$ (dotted) implied by a canonical RBC model under standard quarterly calibration. The histogram in the background plots the time-series distribution of the aggregate capital stock.

Conditional boundary condition In the canonical deterministic neoclassical growth model, the sequential formulation of competitive equilibrium requires a transversality condition to pin down the economically relevant (non-explosive) equilibrium path.[9] The transversality condition rules out unbounded asset accumulation and ensures equivalence between the sequential and recursive formulations.

In this paper, I work directly with a recursive formulation of stochastic equilibrium. Consistency with an underlying sequential economy therefore implicitly imposes a stochastic analogue of transversality. Given the notion of conditional saddle paths, a natural counterpart is *conditional transversality*:

$$\lim_{t\to\infty} \beta^t u'(c_t) K_t = 0 \quad \text{under a frozen aggregate regime } A \in \{B, G\} \qquad (25)$$
$$\text{(along the conditional saddle for each } A \in \{B, G\}).$$

Condition (25) rules out explosive continuations along each conditional saddle and guarantees that the value function remains well defined under the corresponding

[9] This condition is imposed at the aggregate level and should be distinguished from individual no-Ponzi constraints.

frozen-regime dynamics. If, instead, some conditional continuations generated explosive paths, then the recursive representation would cease to be internally consistent because continuation values would be ill behaved along those paths.

Under standard assumptions (e.g. concavity and existence of an optimal plan), (25) is equivalent to the usual stochastic transversality conditions (Kamihigashi, 2003, 2005) on the class of equilibria considered here, in the sense that both select the same bounded recursive competitive equilibrium. The conditional formulation is useful because it makes explicit that the boundary condition operates regime-by-regime along the frozen-regime equilibrium set $\mathcal{M}_A$, a perspective that is essential for the dimension-reduction results that follow.

In the canonical deterministic neoclassical growth model, a transversality condition is needed in the sequential formulation to pin down a unique equilibrium path and to guarantee equivalence between the sequential and recursive formulations.[10] In this paper, I work directly with the recursive formulation and impose (25) as the corresponding stochastic boundary condition, thereby restricting attention to bounded equilibrium paths.

Economies without conditional saddle paths A conditional saddle requires a predetermined endogenous state: without one, the economy jumps each period to the unique bounded allocation implied by the current exogenous state, leaving no nontrivial "along-the-saddle" dynamics.

Remark 1 (Endogenous memorylessness implies degenerate conditional saddle paths)**.** *Consider an RCE with state (Φ_t, A_t). Call the economy endogenously stateless if the endogenous state is memoryless: $\Phi_t = \phi(A_t)$ for some function ϕ, so that all equilibrium allocations depend on A_t only. Then the economy is saddleless: the "conditional steady state" under frozen A is simply $\phi(A)$, and the invariant set is a singleton. Conversely, a non-degenerate conditional saddle requires at least one predetermined endogenous state.*

[10] This condition is imposed at the aggregate level and should be distinguished from individual no-Ponzi constraints.

Example: Gali (2008) three-equation NK model. The textbook New Keynesian model

$$x_t = \mathbb{E}_t x_{t+1} - \tfrac{1}{\sigma}(i_t - \mathbb{E}_t \pi_{t+1} - r_t^n), \tag{26}$$

$$i_t = \varphi_\pi \pi_t + \varphi_x x_t + \nu_t, \tag{27}$$

$$\pi_t = \beta \mathbb{E}_t \pi_{t+1} + \kappa x_t + u_t, \tag{28}$$

under determinacy yields $(x_t, \pi_t, i_t) = \Psi s_t$ for $s_t := (r_t^n, u_t, \nu_t)$ and some matrix Ψ. The equilibrium is endogenously stateless: freezing the exogenous state collapses dynamics to an immediate jump to the conditional steady point. Fluctuations occur entirely *across* conditional points, not along a saddle.

Models with predetermined states—capital, habits, interest-rate smoothing, or distributional states in HANK—are endogenously stateful, and conditional saddle paths generically exist.

3 State dependence in a shock response

In this section, I analyze nonlinear shock responsiveness through the lens of conditional saddle paths. In any stochastic dynamic model that admits conditional saddle paths, a response of an aggregate variable to an exogenous shock is represented by shifts across different conditional saddle paths. Then, if and only if all the conditional saddle paths are parallel along the endogenous state, the response becomes state-independent.

Theorem 1 (State-(in)dependence as a geometric condition)**.**
Fix (Φ_0, A_0) and let $\mathcal{M}(\Phi_0, A_0)$ denote the conditional saddle path under the frozen regime A_0. Let $g(\Phi, A)$ be an aggregate equilibrium object (e.g. consumption) defined for $(\Phi, A) \in \mathcal{M}(\Phi_0, A_0) \times \{A_0, A_1\}$. Define the impact gap between regimes A_1 and A_0 at state Φ by

$$\Delta_g(\Phi; A_1, A_0) := g(\Phi, A_1) - g(\Phi, A_0). \tag{29}$$

Then the following are equivalent:

(i) (State-independent gap) $\Delta_g(\Phi; A_1, A_0)$ is constant on $\mathcal{M}(\Phi_0, A_0)$, i.e. there ex-

ists $c \in \mathbb{R}$ *such that*

$$g(\Phi, A_1) - g(\Phi, A_0) = c \qquad \forall\, \Phi \in \mathcal{M}(\Phi_0, A_0). \tag{30}$$

(ii) (Vertical-translation geometry) Viewed as subsets of $\mathcal{X} \times \mathbb{R}$*,*

$$\mathcal{G}_{A_j} := \{(\Phi, g(\Phi, A_j)) : \ \Phi \in \mathcal{M}(\Phi_0, A_0)\}, \qquad j \in \{0, 1\}, \tag{31}$$

satisfy $\mathcal{G}_{A_1} = \mathcal{G}_{A_0} + (0, c)$*, i.e.* $\mathcal{G}_{A_1}$ *is a constant vertical translation of* $\mathcal{G}_{A_0}$*.*

Proof. $(i) \Rightarrow (ii)$: if $g(\Phi, A_1) = g(\Phi, A_0) + c$ for all Φ, then $(\Phi, g(\Phi, A_1)) = (\Phi, g(\Phi, A_0) + c)$ for all Φ, hence $\mathcal{G}_{A_1} = \mathcal{G}_{A_0} + (0, c)$. $(ii) \Rightarrow (i)$: if $\mathcal{G}_{A_1} = \mathcal{G}_{A_0} + (0, c)$, then for each Φ we must have $g(\Phi, A_1) = g(\Phi, A_0) + c$, so the gap is constant. ■

It is worth noting that both $g(\Phi, A_0)$ and $g(\Phi, A_1)$ are evaluated at the same $\Phi \in M(\Phi_0, A_0)$, while only the regime label varies. Sharp state independence may be a knife-edge property of an RCE. However, Theorem 1 provides an insight regarding conditions under which state dependence becomes amplified. In particular, when a conditional saddle path is more steeply tilted with respect to the endogenous state, as illustrated in Figure 6, a shock responsiveness becomes state dependent. Such differential slopes may arise from various real (Winberry, 2021; Lee, 2025), financial (Melcangi, 2024), labor market frictions (Petrosky-Nadeau et al., 2018; Pizzinelli et al., 2020), and the scope of the relevant shocks include TFP shocks and fiscal/monetary policy shocks (Tenreyro and Thwaites, 2016; Lee, 2025). The sufficiency and the necessity of tilt in the state dependence implies that models with such nature necessarily implies different slopes of the conditional saddle paths.

An example: asymmetric adjustment cost As an example where state dependence arises due to the tilt in the conditional saddle, I consider an extended RBC model with asymmetric adjustment cost. Specifically, the representative household's

budget constraint is modified in the following way:

$$c + a' + \mathcal{C}(a', a) = a(1 + r(X)) + w(X) \tag{32}$$

$$\mathcal{C}(a', a) = \frac{\widetilde{\mu}}{2}\left(\frac{a' - a}{a}\right)^2 a \tag{33}$$

$$\widetilde{\mu} = \begin{cases} \mu_+ & \text{if } a' > a \\ \mu_- & \text{if } a' < a \end{cases} \tag{34}$$

where $\mathcal{C}$ is the wealth adjustment cost which indirectly reflects the frictional capital market. The adjustment cost is asymmetric between positive and negative investment, as specified in equation (34). In particular, I consider the case $\mu_+ > \mu_-$.[11]

Figure 6 plots the conditional saddle paths under asymmetric adjustment costs. Relative to the saddle path associated with A=G, the conditional saddle path for A=B is substantially steeper. As a result, a one–standard-deviation TFP shock generates a larger consumption response when the capital stock is low (3.42%) than when it is high (2.42%).

This geometric representation formalizes the intuition that "climbing up is difficult, falling down is easy"—a recurring theme in the literature on asymmetric business cycles and endogenous disasters (Petrosky-Nadeau et al., 2018). In this framework, asymmetric frictions generate differently tilted conditional saddles: the steeper slope under low productivity implies an aggressive contraction across the conditional saddle paths upon negative shocks, while recovery proceeds more slowly along a flatter path. The resulting gap in shock responsiveness (3.42% versus 2.42% in the example above) arises precisely because the geometric distance between conditional saddles varies with the economy's position along them.

This geometric framework suggests that whenever a model in the literature features endogenous state-dependent dynamics, such behavior must fundamentally originate from the differential tilt of the conditional saddle paths. Theorem 1 establishes that state independence is equivalent to a vertical-translation geometry, in which equilibrium conditional saddle paths remain parallel along the endogenous state. It follows that any deviation into state-dependent responsiveness—regardless of whether the underlying friction is financial, labor-related, or based on adjustment costs—necessarily

[11] The adjustment-cost parameters are not calibrated. For illustrative purposes, I set $\mu_+ = 4$ and $\mu_- = 1$. All other parameters follow a standard quarterly RBC calibration.

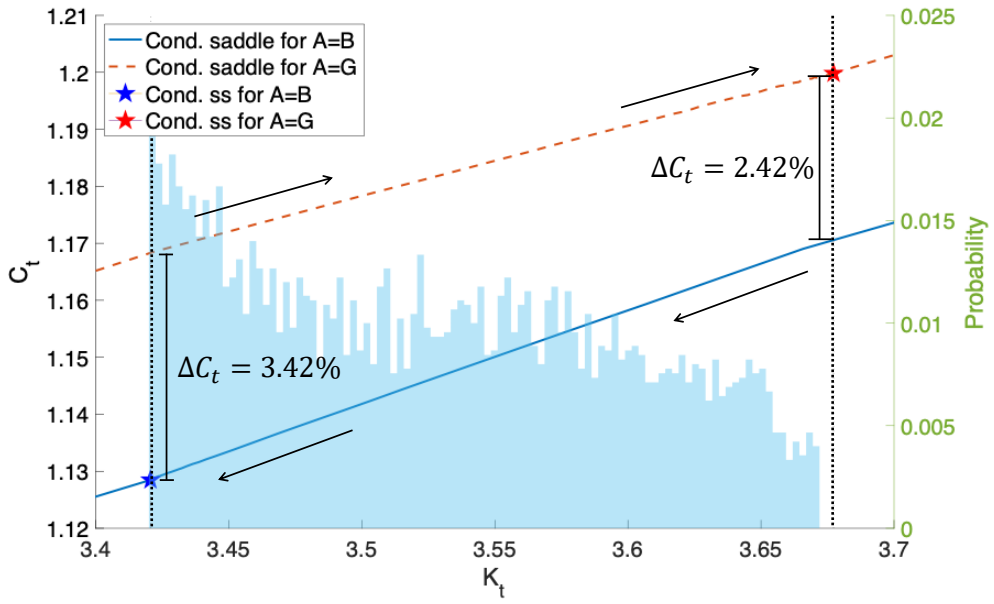

Figure 6: Differently tilted conditional saddle paths – endogenous state dependence

Notes: The figure plots conditional saddle paths for $A = B$ (solid) and $A = G$ (dashed) implied by an RBC model with asymmetric wealth adjustment cost. The conditional saddle path for $A = B$ is steeper than the one for $A = G$. The histogram in the background plots the time-series distribution of the aggregate capital stock.

implies a geometric structure where the local slopes of the conditional saddles diverge across aggregate regimes. In this sense, the "tilt" (the local rate of endogenous accumulation or decumulation) serves as the universal geometric signature of endogenous state dependence.

Furthermore, this framework clarifies the distinction between endogenous and exogenous state dependence. While endogenous state dependence—the sensitivity of shocks to the current endogenous state—necessarily originates from the differential tilt of the conditional saddle paths, exogenous state dependence arises from the interaction and magnitude of the shifts across these paths. Even in economies where saddles are geometrically parallel—resulting in state-independent impact gaps across capital stocks—the equilibrium path may still exhibit nonlinear responses if the exogenous states are "outstretched." In such cases, the vertical distance between saddles reflects a larger exogenous regime shift, creating greater fluctuations that are decomposed into horizontal propagation along the saddles and vertical jumps across them. Consequently, the conditional saddle representation provides a unified visual

tool for assessing both the slope-driven propagation of endogenous frictions and the level-driven impact of exogenous aggregate shocks.

4 Heterogeneous-household economy and dimension reduction

This section introduces conditional saddle path in a canonical heterogeneous-household economy. I consider a continuum of unit measure of ex-ante homogeneous households. The recursive formulation of the households' problem is as follows:

$$v(a, z; \Phi, A) = \max_{c,a'} \quad log(c) + \beta \mathbb{E} v(a', z'; \Phi', A') \tag{35}$$

$$c + a' = a(1 + r(X)) + w(X)z \tag{36}$$

$$a' \geq 0 \tag{37}$$

$$\Phi' = \Gamma_{endo}(\Phi, A), \quad A' \sim \Gamma_{exo}(A'|A). \tag{38}$$

The problem is the same as in the representative-household economy except for 1) uninsurable idiosyncratic labor productivity, which follows a Markov process $z \sim \Gamma_z(z'|z)$; 2) inclusion of distribution of individual states Φ in the aggregate endogenous state; and 3) the corresponding change in the law of motions for the endogenous aggregate state. The RCE is defined as in Krusell and Smith (1998).

The model includes two different stochastic exogenous processes: idiosyncratic productivity and aggregate TFP. Therefore, there are two layers of conditional saddle paths: one is individual conditional saddle path, and the other is aggregate conditional saddle path. The individual saddle path has its own cross-sectional implication which deserves a separate analysis, but it is out of this paper's focus. So, the corresponding analysis is included in Appendix B. I elaborate on the aggregate conditional saddle with stochastic TFP process, where the model closely follows Krusell and Smith (1998).[12] Consistent with the notations in the canonical RBC model in Section 2.2, I denote $K = K(\Phi)$ and $C = C(\Phi_t, A)$ as aggregate capital and consumption.

Based on the law of motion Γ_{endo}, I define conditional K-nullcline as follows:

[12] In the original model of Krusell and Smith (1998), the exogenous individual labor supply co-moves with the exogenous aggregate TFP. All the results stay unaffected after including this feature in the model, but for the expositional brevity, I assume the labor supply is exogenously fixed.

Definition 5 (Conditional K-nullcline in Krusell and Smith (1998))**.**
Fix (Φ_0, A_0) and a regime $A \in \{B, G\}$. Let $\{\Phi_t\}_{t\geq 0}$ be the frozen-regime continuation $\Phi_{t+1} = \Gamma_{\text{endo}}(\Phi_t, A)$. The conditional K-nullcline along the continuation is

$$\mathcal{N}(\Phi_0, A) := \Big\{(K_t, C_t) : \ t \geq 0, \ K(\Gamma_{\text{endo}}(\Phi_t, A)) - K(\Phi_t) = 0\Big\}, \tag{39}$$

where $K_t := K(\Phi_t)$ and $C_t := C(\Phi_t, A)$. When $\mathcal{N}(\Phi_0, A)$ is the graph of a function, define $C_A^{Kcnull}(\cdot; \Phi_0)$ by $\mathcal{N}(\Phi_0, A) = \{(K, C) : \ C = C_A^{Kcnull}(K; \Phi_0)\}$.

Krusell and Smith (1998) posits an endogenous law of motion that tracks aggregate capital K rather than the full distribution Φ: $\log K' = \alpha(A) + \beta(A) \log K$, for $A \in \{B, G\}$, where α and β are state-dependent coefficients. This formulation embeds two distinct assumptions: (i) that aggregate capital K is sufficient to summarize the endogenous aggregate state, and (ii) that K follows a log-linear law of motion. Using the conditional-saddle framework, this paper establishes that (i) is exact: K uniquely indexes the distributional state on the conditional saddle, so conditioning on K entails no loss of information for equilibrium dynamics. By contrast, (ii) remains a parametric approximation—the true law of motion for K is generally non-Markovian and need not be log-linear. The sufficiency result concerns indexing, not the functional form of the law of motion. The following theorem provides the first step toward establishing the exact sufficiency of K.

Theorem 2 (Monotone aggregate variable as a coordinate)**.**
Fix (Φ_0, A_0) and $A \in \{B, G\}$. Let $\{\Phi_t\}_{t\geq 0}$ be the frozen-regime continuation $\Phi_{t+1} = \Gamma_{\text{endo}}(\Phi_t, A)$ and let $\Phi^{cs} := \lim_{t\to\infty} \Phi_t$. Let $e : \mathcal{M}(\Phi_0, A) \to \mathbb{R}$ be an aggregate equilibrium variable. Suppose that the scalar sequence $\{e(\Phi_t)\}_{t\geq 0}$ is strictly monotone and converges to $e(\Phi^{cs})$. Then e uniquely indexes states on the conditional saddle:

$$e(\Phi) = e(\Phi') \implies \Phi = \Phi' \qquad \forall\, \Phi, \Phi' \in \mathcal{M}(\Phi_0, A). \tag{40}$$

Proof. Define $\psi_A : \mathbb{N} \cup \{\infty\} \to \mathcal{M}(\Phi_0, A)$ by $\psi_A(t) := \Phi_t$ for $t \in \mathbb{N}$ and $\psi_A(\infty) := \Phi^{cs}$. By definition of $\mathcal{M}(\Phi_0, A)$ and convergence $\Phi_t \to \Phi^{cs}$, we have

$$\mathcal{M}(\Phi_0, A) = \{\Phi_t : t \geq 0\} \cup \{\Phi^{cs}\}, \tag{41}$$

so ψ_A is surjective. Strict monotonicity of $\{e(\Phi_t)\}$ implies that $e(\Phi_t) \neq e(\Phi_\tau)$ for $t \neq \tau$, hence $\Phi_t \neq \Phi_\tau$ for $t \neq \tau$; therefore ψ_A is injective on $\mathbb{N}$. Moreover, since

$\{e(\Phi_t)\}$ is strictly monotone and converges to $e(\Phi^{cs})$, we also have $e(\Phi_t) \neq e(\Phi^{cs})$ for all finite t, so ψ_A is injective on $\mathbb{N} \cup \{\infty\}$. Thus ψ_A is a bijection between $\mathbb{N} \cup \{\infty\}$ and $\mathcal{M}(\Phi_0, A)$.

Now let $\Phi, \Phi' \in \mathcal{M}(\Phi_0, A)$. Pick $s, s' \in \mathbb{N} \cup \{\infty\}$ such that $\Phi = \psi_A(s)$ and $\Phi' = \psi_A(s')$. If $e(\Phi) = e(\Phi')$, then $e(\psi_A(s)) = e(\psi_A(s'))$. Since $e \circ \psi_A$ is injective, it follows that $s = s'$, hence $\Phi = \Phi'$. Therefore e is injective on $\mathcal{M}(\Phi_0, A)$, and an inverse map φ_A exists on $e(\mathcal{M}(\Phi_0, A))$. ■

Consequently, there exists a unique inverse map $\varphi_A : e(\mathcal{M}(\Phi_0, A)) \to \mathcal{M}(\Phi_0, A)$ such that $\varphi_A(e(\Phi)) = \Phi$ on $\mathcal{M}(\Phi_0, A)$, and any equilibrium object restricted to $\mathcal{M}(\Phi_0, A)$ can be written as a (single-valued) function of the scalar coordinate e.

The intuition behind the theoretical result is as follows: Fix a regime $A \in \{B, G\}$ and restrict attention to the set of equilibrium states that lie on the corresponding conditional saddle (the invariant equilibrium path). Starting from any initial equilibrium state Φ_0 on this set, the equilibrium law of motion determines a unique subsequent sequence $\{\Phi_t\}_{t \geq 0}$ that remains on the invariant conditional saddle path. Then, it converges to the unique conditional steady state. The key geometric observation is that the conditional saddle is effectively a string: it can be viewed as a single curve of equilibrium states. As a consequence, points on the conditional saddle are naturally ordered by their position along this curve.

Now consider the aggregate equilibrium variable e. By assumption, along any equilibrium history on the conditional saddle, the scalar $e_t \equiv e(\Phi_t)$ moves strictly monotonically over time and converges to its conditional steady-state value. Intuitively, e acts as a "progress meter" along the conditional saddle: it always moves in one direction toward its limiting value and never reverses.

Suppose, toward a contradiction, that e were not injective on the conditional saddle. Then there exist two distinct equilibrium states $\Phi \neq \Phi'$ on the conditional saddle such that $e(\Phi) = e(\Phi')$. Consider the two equilibrium histories generated by these initial states. Since both histories begin with the same value of the progress meter and e_t must move strictly one-way toward the same limit along the conditional saddle, the two histories would have to remain synchronized in their progress toward the conditional steady state. But this is impossible because distinct starting points on a one-dimensional conditional saddle generate equilibrium histories that cannot merge. This contradiction implies that no two distinct equilibrium states on the conditional saddle can share the same value of e.

Therefore e uniquely labels equilibrium states on the conditional saddle: if $e(\Phi) = e(\Phi')$, then $\Phi = \Phi'$. This establishes the injectivity claim in Theorem 2 and explains why a strictly monotone, convergent aggregate variable can serve as a one-dimensional indexing variable for equilibrium dynamics on the conditional saddle.

Remark 2 (Injectivity and sufficiency)**.**
Because e is injective on $\mathcal{M}_A$, any equilibrium object restricted to $\mathcal{M}_A$ can be written as a function of (e, A).

Specifically, the following variables can be defined:

$$v^e(\cdot,\cdot;\widetilde{e},A) \in V(\widetilde{e},A) := \{v(\cdot,\cdot;\Phi,A)|\forall\Phi \in \mathcal{M}_A(\Phi_0,A_0) \text{ s.t. } e(\Phi)=\widetilde{e}\} \tag{42}$$

$$r^e(\widetilde{e},A) \in R(\widetilde{e},A) := \{r(\Phi,A)|\forall\Phi \in \mathcal{M}_A(\Phi_0,A_0) \text{ s.t. } e(\Phi)=\widetilde{e}\} \tag{43}$$

$$w^e(\widetilde{e},A) \in W(\widetilde{e},A) := \{w(\Phi,A)|\forall\Phi \in \mathcal{M}_A(\Phi_0,A_0) \text{ s.t. } e(\Phi)=\widetilde{e}\} \tag{44}$$

$$\Gamma^e_{endo}(\widetilde{e},A) \in G(\widetilde{e},A) := \{e\left(\Gamma(\Phi,A)\right)|\forall\Phi \in \mathcal{M}_A(\Phi_0,A_0) \text{ s.t. } e(\Phi)=\widetilde{e}\}. \tag{45}$$

V, R, W and G are nonempty by Assumption 1 and singletons by Theorem 2. Therefore, the recursive problem below is equivalent to the original recursive formulation in equilibrium, as they yield the same equilibrium allocations.

$$v^e(a,z;e,A) = \max_{c,a'} \quad log(c) + \beta\mathbb{E}v^e(a',z';e',A') \tag{46}$$

$$c + a' = a(1 + r^e(e,A)) + w^e(e,A)z \tag{47}$$

$$a' \geq 0 \tag{48}$$

$$e' = \Gamma^e_{endo}(e,A), \quad A' \sim \Gamma_{exo}(A'|A), \tag{49}$$

Now, I show that the conditional K nullclines are the same as in the representative agent model in the following proposition.

Proposition 5 (Conditional K-nullclines of Krusell and Smith (1998))**.**
The heterogeneous household model's conditional K nullclines are identical to the counterparts of the model with the representative household and invariant over the initial distribution Φ_0 and distributional dynamics:

$$C_A^{Kcnull}(K) = AK^\alpha - \delta K, \text{ for } A \in \{B, G\}. \tag{50}$$

Proof.
As in Proposition 3, the stationary condition $\delta K = I$ and the aggregate resource constraint $Y = C + I$ immediately imply the form of the conditional nullclines. ■

Proposition 5 makes the K-nullcline sign-determining: if $C_t < C_A^{Kcnull}(K_t)$ then $\Delta K_t > 0$ and hence $K_{t+1} > K_t$, whereas if $C_t > C_A^{Kcnull}(K_t)$ then $\Delta K_t < 0$ and hence $K_{t+1} < K_t$.

Proposition 6 (K monotonicity and injectivity)**.**
Fix $A \in \{B, G\}$. Under Assumption 1 and Assumption 2, aggregate capital converges to K_A^{cs} strictly monotonically along the frozen-regime continuation on $\mathcal{M}(\Phi_0, A)$. Consequently, K is injective on $\mathcal{M}(\Phi_0, A)$.

Proof.
Fix A and let $\{\Phi_t\}_{t\geq 0}$ be the frozen-regime continuation, with $K_t := K(\Phi_t)$ and $C_t := C(\Phi_t, A)$. By Proposition 5, the conditional K-nullcline is

$$C_A^{Kcnull}(K) = AK^\alpha - \delta K, \tag{51}$$

so along the frozen-regime law of motion,

$$\Delta K_t := K_{t+1} - K_t = C_A^{Kcnull}(K_t) - C_t = -H_t, \tag{52}$$

$$H_t := C_t - C_A^{Kcnull}(K_t). \tag{53}$$

Assumption 2 implies that the line segment connecting (K_t, C_t) and (K_{t+1}, C_{t+1}) does not intersect the nullcline graph, hence

$$H_t H_{t+1} > 0 \qquad \text{for all } t \text{ such that } \Phi_t \neq \Phi^{cs}(\Phi_0, A). \tag{54}$$

Therefore $\{H_t\}$ has a constant sign until convergence, and thus $\Delta K_t = -H_t$ has a constant nonzero sign until convergence. It follows that $\{K_t\}$ is strictly monotone. By Assumption 1(i) and continuity of K,

$$K_t \to K_A^{cs} := K(\Phi^{cs}(\Phi_0, A)). \tag{55}$$

We now apply Theorem 2 with $e(\Phi) = K(\Phi)$ on

$$\mathcal{M}(\Phi_0, A) = \overline{\{\Phi_t : t \geq 0\}}. \tag{56}$$

Since $\{K(\Phi_t)\}_{t\geq 0} = \{K_t\}_{t\geq 0}$ is strictly monotone and converges to $K(\Phi^{cs})$, Theorem 2 implies

$$K(\Phi) = K(\Phi') \implies \Phi = \Phi' \qquad \forall\, \Phi, \Phi' \in \mathcal{M}(\Phi_0, A), \tag{57}$$

i.e. K is injective on $\mathcal{M}(\Phi_0, A)$. ■

Proposition 5 plays a key role in the proof above because it makes the K-nullcline *sign-determining*: the graph $C = C_A^{Kcnull}(K)$ partitions the (K, C) plane into $\Delta K > 0$ and $\Delta K < 0$ regions by $\Delta K = C_A^{Kcnull}(K) - C$. Assumption 2 rules out pathological discrete-time *crossings* of this partition between successive dates by requiring that the line segment connecting (K_t, C_t) and (K_{t+1}, C_{t+1}) does not intersect the nullcline. Together, these two ingredients imply that net investment cannot reverse sign along the conditional saddle, yielding strictly monotone capital dynamics and hence an exact one-dimensional representation indexed by K.

Proposition 6 implies that, conditional on (Φ_0, A), the mapping $K : \mathcal{M}(\Phi_0, A) \to \mathbb{R}$ is one-to-one. Hence there exists an inverse map $\varphi_{\Phi_0,A}$ such that $\Phi = \varphi_{\Phi_0,A}(K(\Phi))$ for all $\Phi \in \mathcal{M}(\Phi_0, A)$.[13] Equivalently, any equilibrium object restricted to $\mathcal{M}(\Phi_0, A)$ admits an exact single-valued representation as a function of (K, A), delivering a one-dimensional state representation along the conditional saddle.

To complement this theoretical result, Figure 7 plots the computed conditional saddle paths in the (K, C) phase diagram. The model is solved globally using the repeated transition method, and the dynamics under each frozen aggregate state are simulated for 2,000 periods. Although the true endogenous state of the model is the full distribution Φ rather than K alone, the figure shows that conditional saddle paths are strictly and monotonically ordered in K, providing clear computational support for the sufficiency result.

From spell-wise to global sufficiency. The reduction result is intentionally regime-by-regime. Proposition 6 establishes that if aggregate capital K is strictly

[13] This is a path-specific notion of sufficiency: for a fixed (Φ_0, A), K uniquely indexes states on the entire conditional saddle $\mathcal{M}(\Phi_0, A)$ (i.e. globally *along the transition path*).

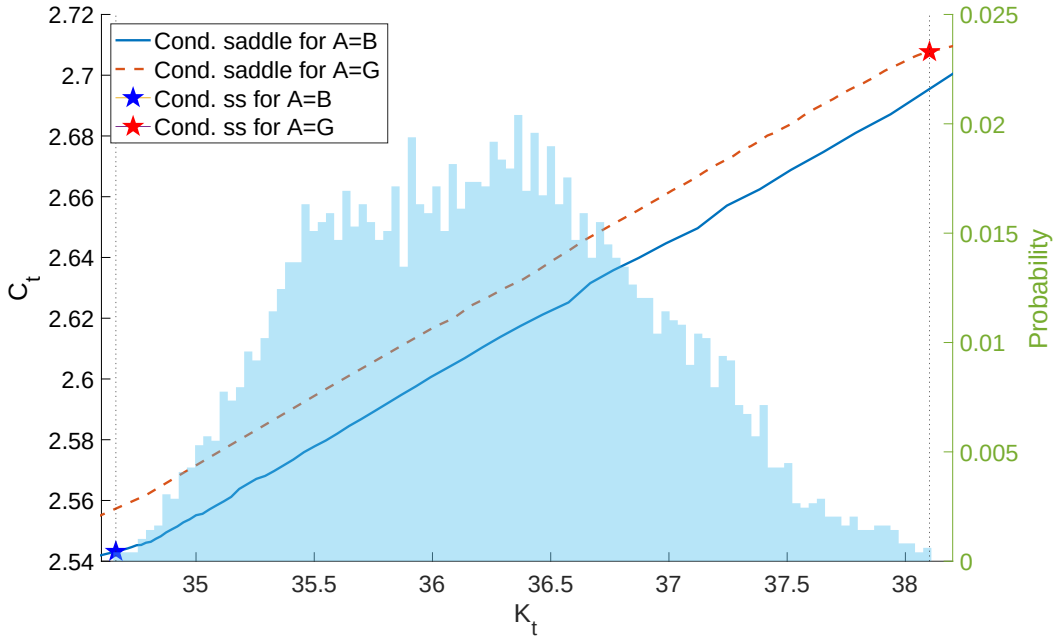

Figure 7: Conditional saddle paths in Krusell and Smith (1998)

Notes: The figure plots conditional saddle paths for $A = B$ (solid) and $A = G$ (dashed) implied by a canonical heterogeneous household business cycle model (Krusell and Smith, 1998). The histogram in the background plots the time-series distribution of the aggregate capital stock.

monotone along the frozen-regime continuation, it uniquely indexes the entire conditional saddle $\mathcal{M}(A; \Phi_0)$. This is global along the transition set, not a local or linearized statement. Under regime switching, the economy is not confined to one frozen saddle forever. Instead, time decomposes into regime spells:

- Within a spell, the economy evolves along a saddle path monotonically indexed by K.
- At a switch (period τ), the current state Φ_τ becomes the entry condition for the next frozen-regime continuation under the new regime A_τ.
- By Proposition 6, the subsequent sequence $\{K_t\}_{t \geq \tau}$ is again strictly monotone along that continuation, so K provides an exact coordinate on the new conditional saddle $\mathcal{M}(\Phi_\tau; A_\tau)$.

Thus, a regime switch does not break the reduction; it restarts it. Along any realized regime history, the equilibrium path is a concatenation of one-dimensional segments,

and (K_t, A_t) is an exact sufficient statistic for the equilibrium set that the economy evolves along. Crucially, "conditioning on Φ_0" defines the current manifold—it does not imply that agents carry Φ_0 as a state variable. At each regime switch, the entry condition updates to Φ_τ, which is already uniquely indexed by K_τ from the previous spell. The "handoff" between spells is pinned down by (K, A), so no additional infinite-dimensional tracking is required.

From near rationality to complete rationality Krusell and Smith (1998) assumes the specific parametric law of motion to compute the heterogeneous-household model. Then, they confirm the accuracy of the law of motion through the accurate consistency between the realized and assumed dynamics. After the celebrated contribution, the approach is often labeled as near or bounded rational approach. The conditional-saddle framework shows that, restricted to the conditional saddle, conditioning on K can be exact (a sufficient statistic) for equilibrium objects. The additional log-linear functional form used by Krusell and Smith (1998) remains a quantitative approximation.

Parametric form of the conditional saddle paths Despite the indexing function K, specific conditional saddle paths and the form of the law of motion remains undetermined. This problem exists even for representative agent business cycle models. Lee (2025) develops repeated transition method that utilizes the recurrence of the equilibrium allocations along the conditional saddle path. For heterogeneous-agent models, the existence of the indexing variable (sufficient statistic) starkly eases the implementation of the RTM. Theorem 2 and Proposition 6 theoretically supports the implementation feasibility of the RTM using the sufficient statistic.

4.1 Primitive conditions for Assumption 2

This section provides primitive sufficient conditions under which Assumption 2 holds in the heterogeneous-household economy of Krusell and Smith (1998). Assumption 2 rules out discrete-time "side-switching" across this partition between dates (equivalently, it prevents the straight segment joining consecutive points (K_t, C_t) and (K_{t+1}, C_{t+1}) from intersecting the nullcline). The results below show that such side-switching is excluded under economically interpretable bounds on households'

marginal propensities to consume and sufficiently weak general-equilibrium price feedback.

Household MPC bounds Let $c(a, z; r, w)$ denote the stationary equilibrium household consumption policy as a function of individual assets a, idiosyncratic state $z \in \mathcal{Z}$, and prices (r, w). Along a frozen-regime continuation, aggregate consumption can change with aggregate capital because K affects prices, which in turn affects contemporaneous income components wz and ra. A convenient "MPC bound" in this context is therefore a bound on the *marginal response of consumption to price-induced changes in current income*, rather than an MPC out of an exogenous transfer shock.

Assumption 3 (Bounded price-income MPC)**.**
Along the frozen-regime continuation under A, there exists $\bar{m} \in (0, 1)$ such that for the stationary equilibrium policy $c(a, z; r, w)$,

$$0 \leq \frac{\partial c}{\partial (wz)}(a, z; r, w) \leq \bar{m}, \qquad 0 \leq \frac{\partial c}{\partial (ra)}(a, z; r, w) \leq \bar{m}, \tag{58}$$

for all (a, z) in the support of Φ_t and all t on the continuation.[14]

Under Assumption 3, a marginal increase in aggregate capital affects contemporaneous aggregate consumption through the induced changes in wages and returns. Define the (pathwise) bounds as

$$\bar{Z} := \sup_{t \geq 0} \int z \, d\Phi_t, \qquad \bar{a} := \sup_{t \geq 0} \int a \, d\Phi_t, \qquad \mathcal{K} := \{K_t : t \geq 0\}. \tag{59}$$

Then, the change in aggregate consumption induced by a marginal change in K can be bounded above by the aggregate MPC bound $\bar{m}$ times the induced change in contemporaneous labor and capital incomes.

[14] Assumption 3 bounds the marginal response of consumption to *price-induced* changes in contemporaneous income components. This local derivative bound differs from the standard MPC out of a transitory transfer. In incomplete-markets environments, precautionary saving and borrowing constraints typically prevent one-for-one consumption responses to marginal changes in current income, making an upper bound $\bar{m} < 1$ natural on the relevant region of the state space.

Sufficient condition for Assumption 2. In the Krusell–Smith benchmark with Cobb–Douglas production, prices are smooth functions of K:

$$w_A(K) = (1-\alpha)AK^{\alpha}, \qquad r_A(K) = \alpha AK^{\alpha-1} - \delta, \tag{60}$$

with derivatives

$$w_A'(K) = (1-\alpha)\alpha AK^{\alpha-1}, \qquad r_A'(K) = \alpha(\alpha-1)AK^{\alpha-2}. \tag{61}$$

Moreover, the nullcline satisfies $\big(C_A^{Kcnull}\big)'(K) = \alpha AK^{\alpha-1} - \delta$. The next lemma shows that if general-equilibrium price feedback is sufficiently weak relative to the nullcline slope, then the nullcline gap H_t cannot change sign, which implies Assumption 2 along the continuation.

Lemma 1 (Sufficient condition for Assumption 2)**.**
Fix $A \in \{B, G\}$ and consider the frozen-A continuation $\{\Phi_t\}_{t\geq 0}$ with $K_t := K(\Phi_t)$ and $C_t := C(\Phi_t, A)$. Under Assumption 3, suppose that along $\mathcal{K}$,

$$\sup_{K\in\mathcal{K}} \Big(\bar{m}\big(w_A'(K)\,\bar{Z} + |r_A'(K)|\,\bar{a}\big) - \big(C_A^{Kcnull}\big)'(K) \Big) \;<\; 1. \tag{62}$$

Then $H_t H_{t+1} > 0$ for all t such that $\Phi_t \neq \Phi^{cs}(\Phi_0, A)$, and hence Assumption 2 holds along the continuation. Consequently, $\{K_t\}$ is strictly monotone until convergence.

Proof.
Define the nullcline gap $H_t := C_t - C_A^{Kcnull}(K_t)$ so that $\Delta K_t := K_{t+1} - K_t = -H_t$. A mean-value expansion yields, for some ξ_t between K_t and K_{t+1},

$$H_{t+1} - H_t = \big(C_{t+1} - C_t\big) - \Big(C_A^{Kcnull}(K_{t+1}) - C_A^{Kcnull}(K_t)\Big) \tag{63}$$

$$= \Big(\frac{dC}{dK}(\xi_t) - \big(C_A^{Kcnull}\big)'(\xi_t)\Big)\,(K_{t+1} - K_t). \tag{64}$$

By Assumption 3, the induced change in aggregate consumption from a marginal increase in K is bounded above by the aggregate MPC bound times the induced

change in contemporaneous incomes:

$$\frac{dC}{dK}(\xi_t) \le \bar{m}\Big(w'_A(\xi_t)\int z\, d\Phi_t + |r'_A(\xi_t)|\int a\, d\Phi_t\Big) \tag{65}$$

$$\le \bar{m}\big(w'_A(\xi_t)\bar{Z} + |r'_A(\xi_t)|\bar{a}\big). \tag{66}$$

Using $K_{t+1} - K_t = -H_t$ gives

$$H_{t+1} = \Big[1 - \Big(\frac{dC}{dK}(\xi_t) - \big(C_A^{Kcnull}\big)'(\xi_t)\Big)\Big]H_t. \tag{67}$$

Condition (62) implies that the bracketed multiplier is strictly positive for all t, hence $\{H_t\}$ cannot change sign: $H_t H_{t+1} > 0$ for all pre-limit t. Therefore $\Delta K_t = -H_t$ has constant nonzero sign, so $\{K_t\}$ is strictly monotone until convergence. ■

A local check near the conditional steady state. The global bound (62) can be weakened to a neighborhood condition near the conditional steady state. This is useful both for economic interpretation and for quantitative verification in standard calibrations.

Corollary 1 (A local check near K_A^{cs})**.**
Under Assumption 3, suppose there exists $\varepsilon > 0$ such that the continuation satisfies $K_t \in (K_A^{cs} - \varepsilon, K_A^{cs} + \varepsilon)$ for all sufficiently large t, and

$$\sup_{|K - K_A^{cs}| \le \varepsilon} \Big(\bar{m}\big(w'_A(K)\,\bar{Z} + |r'_A(K)|\,\bar{a}\big) - \big(C_A^{Kcnull}\big)'(K)\Big) \;<\; 1. \tag{68}$$

Then there exists $T < \infty$ such that $H_t H_{t+1} > 0$ (and hence Assumption 2) holds for all $t \ge T$, implying that K_t is eventually strictly monotone and converges to K_A^{cs} without side-switching.

Proof.
The proof follows Lemma 1, restricting attention to $t \ge T$ such that $K_t \in [K_A^{cs} - \varepsilon, K_A^{cs} + \varepsilon]$ and applying the local bound (68). ■

Conditions (62)–(68) are directly checkable in quantitative implementations: one evaluates the left-hand side along a simulated frozen-regime continuation using the model-implied bound $\bar{m}$ and the moments $\bar{Z}$ and $\bar{a}$. In standard Krusell–Smith cal-

ibrations, K moves slowly and the general-equilibrium price feedback terms $w'_A(K)$ and $|r'_A(K)|$ are modest, so the inequalities are typically satisfied with slack.[15]

4.2 Extensions

Theorem 2 provides verifiable conditions for dimension reduction: identify the K-nullcline and verify monotonicity. This section applies the diagnostic to several extensions, illustrating both the framework's scope and its limits.

Economies with multiple endogenous states Theorem 2 applies to an economy with the multivariate (distributional) endogenous state. As long as there is an aggregate equilibrium variable e that strictly monotonically converges to the conditional steady-state level, then e is a sufficient statistic.

For example, consider the following model that extends the heterogeneous-agent model above by adding endogenous bond holding. The following is the corresponding budget constraint:

$$c + a' + q(\Phi, A)b' = a(1 + r(\Phi, A)) + b + w(\Phi, A)z \tag{69}$$

where b is bond holding and q is the bond price competitively determined by

$$\int b'(a, z; \Phi, A)d\Phi = 0. \tag{70}$$

The key observation is that Proposition 5 continues to hold: the conditional K-nullcline remains $C_A^{K\text{-null}}(K) = AK^\alpha - \delta K$, determined solely by the aggregate resource constraint. Since bonds are in zero net supply, their inclusion does not alter the sign-determining property of the nullcline. Thus, the monotonicity argument of Proposition 6 applies, and K remains a sufficient statistic. Lee (2025) showed that the equilibrium allocations are strictly monotonically sorted along K through the globally solved computational outcome. This is because the conditional saddle's strict monotone property along K implied by its conditional nullcline is unaffected by the inclusion of bond dimension. It confirms the prediction of Theorem 2.

[15] In the baseline KS98 calibration, the left-hand side of (62) evaluated along the simulated frozen-A continuation is around 0.05 even under the conservative envelope $\bar{m} = 1$, well below the threshold 1.

Models with endogenous labor supply A heterogeneous-household model with endogenous labor supply and CRRA–GHH preferences is a natural extension of the exogenous-labor-supply framework studied in this paper. GHH utility is particularly useful in this context because it eliminates wealth effects in labor-supply decisions, which could otherwise disrupt the monotonicity properties through distributional channels. Consider preferences given by

$$u(c, l_H) = \frac{1}{1-\sigma}\left(c - \frac{\eta}{1+\frac{1}{\chi}} l_H^{1+\frac{1}{\chi}}\right)^{1-\sigma}, \tag{71}$$

and the budget constraint

$$c + a' = a(1 + r(\Phi, A)) + w(\Phi, A) z l_H, \tag{72}$$

where z denotes idiosyncratic labor productivity. The individual labor-supply optimality condition then implies the following aggregate labor supply $L(\Phi, A)$:

$$l_H(a, z; \Phi, A) = \left(\frac{z}{\eta}\right)^{\chi} w(\Phi, A)^{\chi} \tag{73}$$

$$L(\Phi, A) = \int z l_H(a, z; \Phi, A) d\Phi = w(\Phi, A)^{\chi} \int \frac{z^{\chi+1}}{\eta^{\chi}} d\Phi_z \tag{74}$$

where $M = \int \frac{z^{\chi+1}}{\eta^{\chi}} d\Phi_z$ and Φ_z is the cumulative distribution function of the stationary productivity distribution. Then, from the optimality condition in the production sector with respect to the labor demand,

$$(1-\alpha) A K^{\alpha} L(\Phi, A)^{-\alpha} = w(\Phi, A) = \left(\frac{L(\Phi, A)}{M}\right)^{\frac{1}{\chi}}. \tag{75}$$

Combining these two conditions, the conditional aggregate capital nullcline is as follows:

$$c_A^{Kcnull} = A(M^{\frac{1}{1+\alpha\chi}}((1-\alpha)A)^{\frac{\chi}{1+\alpha\chi}})^{1-\alpha}(K_A^{Kcnull})^{\alpha+(1-\alpha)\frac{\alpha\chi}{1+\alpha\chi}} - \delta K_A^{Kcnull}, \tag{76}$$

which satisfies the same monotone convergence to the conditional steady state.

Distributional disturbance Now consider the following CRRA-utility setup:

$$u(c, l_H) = \frac{1}{1-\sigma} c^{1-\sigma} - \frac{\eta}{1+\frac{1}{\chi}} l_H^{1+\frac{1}{\chi}}. \tag{77}$$

The corresponding individual labor supply is as follows:

$$l_H(a, z; \Phi, A) = \left(\frac{z}{\eta c(a, z; \Phi, A)^{\sigma}} \right)^{\chi} w(\Phi, A)^{\chi} \tag{78}$$

Following the same step as in the GHH case above, I obtain the following conditional K nullcline condition:

$$c_A^{Kcnull} = A(M(\Phi^{Kcnull})^{\frac{1}{1+\alpha\chi}}((1-\alpha)A)^{\frac{\chi}{1+\alpha\chi}})^{1-\alpha}(K_A^{Kcnull})^{\alpha+(1-\alpha)\frac{\alpha\chi}{1+\alpha\chi}} - \delta K_A^{Kcnull}, \tag{79}$$

where $M(\Phi^{Kcnull}) = \int \frac{z^{\chi+1}}{\eta^{\chi} c^{\sigma\chi}} d\Phi^{Kcnull}$. Because of heterogeneous wealth effects, the conditional capital nullcline depends on the distribution of individual states Φ^{Kcnull} associated with the level K^{cnull}. As a result, strict monotonicity of the capital dynamics cannot be verified analytically. Nevertheless, Lee (2025) provides computational evidence that the recursive competitive equilibrium of the model with this utility specification exhibits strictly monotone convergence of aggregate capital K under the standard calibration.

4.3 Further applications

The conditional saddle framework extends beyond the neoclassical setting.[16] We briefly illustrate the framework in a search-and-matching environment, where the predetermined state is unemployment and the conditional saddle paths recover the Beveridge curve as a regime-specific transition locus.

Search and matching Consider a discrete-time stochastic Diamond–Mortensen–Pissarides economy.[17] Aggregate productivity follows a two-state Markov chain $z \in$

[16] Companion work applies conditional saddle paths to New Keynesian models with an occasionally binding zero lower bound (Lee and Nomura, 2026) and to production network economies with endogenous linkage formation (Lee and Sun, 2026).

[17] The full model specification is in Appendix D. We adopt a standard formulation following Shimer (2005) with Nash-bargained wages, exogenous separation, and Cobb–Douglas matching.

$\{G, B\}$. The aggregate state is $S = [u_{-1},\, z]$, where unemployment $u_{-1} = 1 - n_{-1}$ is the sole predetermined endogenous state. Employment evolves according to

$$n \;=\; (1-\lambda)\, n_{-1} \;+\; q(\theta)\,(1-n_{-1}), \tag{80}$$

where $\lambda \in (0,1)$ is the exogenous separation rate, $\theta = v/u$ is labor market tightness, and $q(\theta) = m\theta^{-\xi}$ is the vacancy-filling probability implied by a Cobb–Douglas matching function. Market tightness $\theta(S)$—and hence vacancies $v(S) = \theta(S) \cdot u_{-1}$—is the jump variable, pinned down by the free-entry condition for vacancy posting:

$$\frac{\kappa}{q(S)} \;=\; (1-\lambda)\,\beta\,\mathbb{E}\left[\left(\frac{c(S)}{c(S')}\right)^{\sigma}\left(z' - w(S') + \frac{\kappa}{q(S')}\right)\,\middle|\, S\right], \tag{81}$$

where κ is the vacancy posting cost, $w(S)$ is the Nash-bargained wage, and $c(S) = n(S)\,z - \kappa\,v(S) + (1-n(S))\,b$ is aggregate consumption from the resource constraint.

The conditional saddle path $\mathcal{M}(z;\, u_0)$ is the orbit $\{(u_t, v_t)\}_{t\geq 0}$ generated by (80) and the equilibrium vacancy function $v(\cdot, z)$ under frozen productivity z, with limit point $(u_z^{\text{cs}}, v_z^{\text{cs}})$.

Slope asymmetry and the Beveridge curve. Figure 8 plots the conditional saddle paths in (u_{-1}, v) space. Both loci slope upward—higher inherited unemployment raises equilibrium vacancies regardless of the regime, since more slack means more unfilled matches to exploit—so state dependence is sign-preserving, as in the RBC benchmark. However, the slopes differ markedly. Under G, the conditional saddle is steeply sloped: each unit of inherited slack generates aggressive vacancy posting because matches are highly profitable. Under B, the saddle is nearly flat: vacancy posting collapses and barely responds to the unemployment state, because the flow surplus from a match is too low to justify the posting cost.

This slope asymmetry provides a geometric characterization of the labor market's asymmetric response to aggregate shocks. Consider the economy starting near the G conditional steady state $(u_G^{\text{cs}}, v_G^{\text{cs}})$—low unemployment, moderate vacancies. A negative productivity shock switches the economy onto the B conditional saddle at the same inherited u_{-1}. Because the B saddle is nearly flat at this unemployment level, vacancies collapse on impact. As the economy subsequently evolves along the flat B saddle toward $(u_B^{\text{cs}}, v_B^{\text{cs}})$, unemployment accumulates but vacancies barely adjust—the

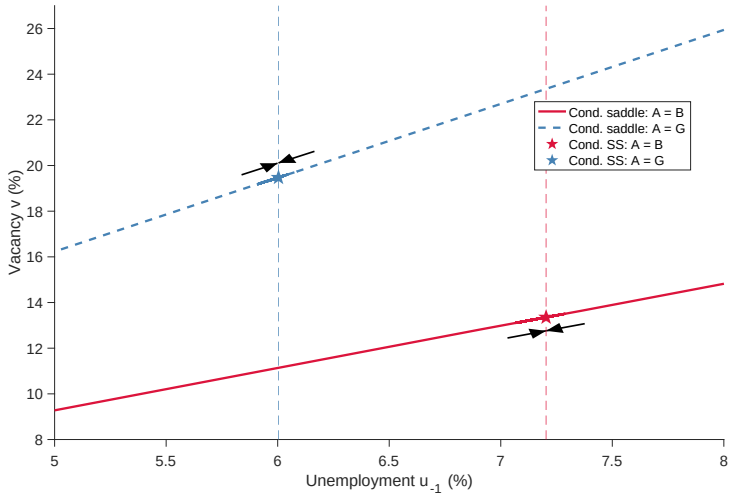

Figure 8: Conditional saddle paths in the DMP model

Notes: The figure plots conditional saddle paths in (u_{-1}, v) space, computed by freezing aggregate productivity at $z = G$ (dashed blue) or $z = B$ (solid red) and simulating the frozen-regime continuation under the globally solved equilibrium mappings. Stars mark the regime-specific conditional steady states. Dashed vertical lines indicate the conditional steady-state unemployment levels. Direction arrows show the frozen-regime convergence along each conditional saddle. Both loci slope upward (sign-preserving state dependence), but the G saddle is an order of magnitude steeper than the B saddle: inherited slack generates aggressive vacancy posting in expansions but elicits almost no response in recessions.

labor market is sluggish in the downturn. Conversely, when productivity recovers and the economy switches from the flat B saddle back to the steep G saddle at high inherited u_{-1}, vacancies spike sharply, driving rapid job creation. Recoveries are fast precisely because the G saddle is steep where the B saddle deposits the economy.

The Beveridge curve "loop" observed in empirical (u, v) data—the counterclockwise rotation through recessions and recoveries—is thus the across-saddle jump dynamics of the stochastic equilibrium: a vertical drop from the steep to the flat saddle entering recession, a rightward drift along the flat saddle during the downturn, and a vertical jump back onto the steep saddle when productivity returns.

5 Concluding remarks

This paper develops a geometric framework for stochastic equilibrium dynamics by introducing *conditional saddle paths*: invariant equilibrium paths defined under frozen exogenous states. This object extends the familiar saddle-path intuition from deter-

ministic models to environments under aggregate uncertainty. In the resulting phase-diagram representation, business-cycle fluctuations decompose into movements *along* a conditional saddle (endogenous propagation within a regime) and *across* conditional saddles (transitions in exogenous states). The framework clarifies why impulse responses can be state-dependent: such dependence is a geometric property of the stable equilibrium branch and arises precisely when conditional saddles differ in slope rather than by mere vertical translation.

When an aggregate equilibrium variable varies strictly monotonically along a conditional saddle, it provides a global coordinate: it uniquely indexes equilibrium states and therefore summarizes all equilibrium allocations and prices on the relevant invariant set. Applying this logic, I provide a theoretical proof of the sufficiency of aggregate capital in a canonical heterogeneous-household model. Beyond the Krusell–Smith benchmark, the same reasoning applies in multi-asset and richer heterogeneous-agent environments whenever a monotone-convergent aggregate coordinate exists.

More broadly, conditional saddles offer a complementary lens on stochastic models: they provide a language for interpreting nonlinear dynamics and for assessing when scalar state approximations are exact rather than merely accurate. They also provide a natural geometry for *state-contingent* policy analysis: by making state dependence explicit in the phase diagram, the framework clarifies when the same intervention should be expected to have different quantitative effects across regimes and over the cycle. A promising direction for future work is to use these geometric objects to sharpen empirical restrictions on state dependence and to discipline the design of state-contingent stabilization policies in heterogeneous-agent economies under aggregate uncertainty.

References

Achdou, Y., J. Han, J.-M. Lasry, P.-L. Lions, and B. Moll (2021, 04). Income and wealth distribution in macroeconomics: A continuous-time approach. *The Review of Economic Studies 89*(1), 45–86.

Ahn, S., G. Kaplan, B. Moll, T. Winberry, and C. Wolf (2018). When Inequality Matters for Macro and Macro Matters for Inequality. *NBER Macroeconomics Annual 32*, 1–75. _eprint: https://doi.org/10.1086/696046.

Algan, Y., O. Allais, and W. J. Den Haan (2008). Solving heterogeneous-agent models with parameterized cross-sectional distributions. *Journal of Economic Dynamics and Control 32*(3), 875–908.

Algan, Y., O. Allais, and W. J. Den Haan (2010). Solving the incomplete markets model with aggregate uncertainty using parameterized cross-sectional distributions. *Journal of Economic Dynamics and Control 34*(1), 59–68. Computational Suite of Models with Heterogeneous Agents: Incomplete Markets and Aggregate Uncertainty.

Andreasen, M. M., J. Fernández-Villaverde, and J. F. Rubio-Ramírez (2017, 06). The pruned state-space system for non-linear dsge models: Theory and empirical applications. *The Review of Economic Studies 85*(1), 1–49.

Arnold, L. (1998). *Random Dynamical Systems*. Springer Monographs in Mathematics. Berlin, Heidelberg: Springer Berlin Heidelberg.

Auclert, A., B. Bardóczy, M. Rognlie, and L. Straub (2021). Using the sequence-space jacobian to solve and estimate heterogeneous-agent models. *Econometrica 89*(5), 2375–2408.

Azinovic, M., L. Gaegauf, and S. Scheidegger (2022). Deep equilibrium nets. *International Economic Review 63*(4), 1471–1525.

Baley, I. and A. Blanco (2019, January). Firm uncertainty cycles and the propagation of nominal shocks. *American Economic Journal: Macroeconomics 11*(1), 276–337.

Basu, S. and B. Bundick (2017). Uncertainty shocks in a model of effective demand. *Econometrica 85*(3), 937–958.

Berger, D., K. Milbradt, F. Tourre, and J. Vavra (2021, September). Mortgage prepayment and path-dependent effects of monetary policy. *American Economic Review 111*(9), 2829–78.

Berger, D. and J. Vavra (2015, January). Consumption Dynamics During Recessions: Consumption Dynamics During Recessions. *Econometrica 83*(1), 101–154.

Bloom, N., M. Floetotto, N. Jaimovich, I. Saporta-Eksten, and S. J. Terry (2018). Really Uncertain Business Cycles. *Econometrica 86*(3), 1031–1065.

Boppart, T., P. Krusell, and K. Mitman (2018, April). Exploiting MIT shocks in heterogeneous-agent economies: the impulse response as a numerical derivative. *Journal of Economic Dynamics and Control 89*, 68–92.

Bourany, T. (2018). Wealth distribution over the business cycle: A mean-field game with common noise. Master's thesis, UPMC-Sorbonne Université. Supervised by Yves Achdou, Paris-Diderot University (LJLL).

Cao, D., W. Luo, and G. Nie (2023, January). Global DSGE Models. *Review of Economic Dynamics*, S1094202523000017.

Cass, D. (1965, 07). Optimum growth in an aggregative model of capital accumulation1. *The Review of Economic Studies 32*(3), 233–240.

Dechert, W. D. and K. Nishimura (1983). A complete characterization of optimal growth paths in an aggregated model with a non-concave production function. *Journal of Economic Theory 31*(2), 332–354.

Den Haan, W. J. (1996). Heterogeneity, aggregate uncertainty, and the short-term interest rate. *Journal of Business & Economic Statistics 14*(4), 399–411.

Den Haan, W. J. (1997). Solving Dynamic Models with Aggregate Shocks and Heterogeneous Agents. *Macroeconomic Dynamics 1*(2), 355–386. Publisher: Cambridge University Press.

Den Haan, W. J. and A. Marcet (1990). Solving the stochastic growth model by parameterizing expectations. *Journal of Business & Economic Statistics 8*(1), 31–34.

Den Haan, W. J. and P. Rendahl (2010, January). Solving the incomplete markets model with aggregate uncertainty using explicit aggregation. *Journal of Economic Dynamics and Control 34*(1), 69–78.

Elenev, V., T. Landvoigt, and S. Van Nieuwerburgh (2021). A Macroeconomic Model With Financially Constrained Producers and Intermediaries. *Econometrica 89*(3), 1361–1418.

Fernández-Villaverde, J., S. Hurtado, and G. Nuño (2023). Financial frictions and the wealth distribution. *Econometrica 91*(3), 869–901.

Gali, J. (2008). *Monetary Policy, Inflation, and the Business Cycle: An Introduction to the New Keynesian Framework and Its Applications*. Princeton University Press.

Han, J., Y. Yang, and W. E (2025). DeepHAM: A Global Solution Method for Heterogeneous Agent Models with Aggregate Shocks. Working Paper.

Kamihigashi, T. (2003). Necessity of transversality conditions for stochastic problems. *Journal of Economic Theory 109*(1), 140–149.

Kamihigashi, T. (2005). Necessity of the transversality condition for stochastic models with bounded or crra utility. *Journal of Economic Dynamics and Control 29*(8), 1313–1329.

Kaplan, G., B. Moll, and G. L. Violante (2018, March). Monetary policy according to hank. *American Economic Review 108*(3), 697–743.

Kaplan, G. and G. L. Violante (2014). A model of the consumption response to fiscal stimulus payments. *Econometrica 82*(4), 1199–1239.

Khan, A. and J. K. Thomas (2013). Credit shocks and aggregate fluctuations in an economy with production heterogeneity. *Journal of Political Economy 121*(6), 1055–1107.

Koop, G., M. Pesaran, and S. M. Potter (1996). Impulse response analysis in nonlinear multivariate models. *Journal of Econometrics 74*(1), 119–147.

Koopmans, T. (1963). On the concept of optimal economic growth. Cowles Foundation Discussion Papers 163, Cowles Foundation for Research in Economics, Yale University.

Krusell, P. and A. A. Smith, Jr. (1997, June). Income and Wealth Heterogeneity, Portfolio Choice, and Equilibrium Asset Returns. *Macroeconomic Dynamics 1*(02).

Krusell, P. and A. A. Smith, Jr. (1998, October). Income and Wealth Heterogeneity in the Macroeconomy. *Journal of Political Economy 106*(5), 867–896.

Lee, H. (2025). Global nonlinear solutions in sequence space and the generalized transition function. Working Paper.

Lee, H. (2026). Striking While the Iron Is Cold: Fragility after a Surge of Lumpy Investments. *Working Paper*, 68.

Lee, H. and K. Nomura (2026). The Spender of Last Resort: Global Equilibrium Dynamics under the Zero Lower Bound. Working Paper.

Lee, H. and Y. Sun (2026). Endogenous Plucking Through Networks: The Plucking Paradox. Working Paper.

Marcet, A. (1988). Solving nonlinear stochastic models by parameterizing expectations. Manuscript. Pittsburgh: Carnegie Mellon Univ.

Melcangi, D. (2024). Firms' precautionary savings and employment during a credit crisis. *American Economic Journal: Macroeconomics 16*(1), 356–386.

Mendoza, E. G. (2010, December). Sudden stops, financial crises, and leverage. *American Economic Review 100*(5), 1941–66.

Payne, J., A. Rebei, and Y. Yang (2025). Deep Learning for Search and Matching Models. Working Paper.

Petrosky-Nadeau, N., L. Zhang, and L.-A. Kuehn (2018, August). Endogenous disasters. *American Economic Review 108*(8), 2212–45.

Pizzinelli, C., K. Theodoridis, and F. Zanetti (2020). State dependence in labor market fluctuations. *International Economic Review 61*(3), 1027–1072.

Proehl, E. (2025). Existence and Uniqueness of Recursive Equilibria with Aggregate and Idiosyncratic Risk. Working Paper.

Ramsey, F. P. (1928, 12). A mathematical theory of saving. *The Economic Journal 38*(152), 543–559.

Reddy, P. B., J. M. Schumacher, and J. C. Engwerda (2020). A Bendixson criterion for optimal control of a class of hybrid systems. *SIAM Journal on Control and Optimization 58*(4), 2219–2252.

Reiter, M. (2001, April). Recursive Solution Of Heterogeneous Agent Models. Computing in Economics and Finance 2001 167, Society for Computational Economics.

Reiter, M. (2010). Solving the incomplete markets model with aggregate uncertainty by backward induction. *Journal of Economic Dynamics and Control 34*(1), 28–35. Computational Suite of Models with Heterogeneous Agents: Incomplete Markets and Aggregate Uncertainty.

Schenk-Hoppé, K. R. (2001). Random dynamical systems in economics. *Stochastics and Dynamics*.

Schenk-Hoppé, K. R. and B. Schmalfuß (2001). Random fixed points in a stochastic solow growth model. *Journal of Mathematical Economics 36*(1), 19–30.

Schenk-Hoppé, K. R. (1998). Random attractors–general properties, existence and applications to stochastic bifurcation theory. *Discrete and Continuous Dynamical Systems 4*(1), 99–130.

Shimer, R. (2005, March). The cyclical behavior of equilibrium unemployment and vacancies. *American Economic Review 95*(1), 25–49.

Skiba, A. K. (1978). Optimal growth with a convex–concave production function. *Econometrica 46*(3), 527–539.

Solow, R. M. (1956). A contribution to the theory of economic growth. *The Quarterly Journal of Economics 70*(1), 65–94.

Swan, T. W. (1956). Economic growth and capital accumulation. *Economic Record 32*(2), 334–361.

Tenreyro, S. and G. Thwaites (2016, October). Pushing on a String: US Monetary Policy Is Less Powerful in Recessions. *American Economic Journal: Macroeconomics 8*(4), 43–74.

Vavra, J. (2014). Inflation dynamics and time-varying volatility: New evidence and an ss interpretation. *The Quarterly Journal of Economics 129*(1), 215–258.

Wagener, F. (2003). Skiba points and heteroclinic bifurcations, with applications to the shallow lake system. *Journal of Economic Dynamics and Control 27*(9), 1533–1561.

Walsh, K. J. and E. Young (2024). Equilibrium multiplicity in aiyagari and krusell-smith. Working paper.

Winberry, T. (2021, January). Lumpy Investment, Business Cycles, and Stimulus Policy. *American Economic Review 111*(1), 364–396.

Yannacopoulos, A. N. (2011). Stochastic saddle paths and economic theory. In M. M. Peixoto, A. A. Pinto, and D. A. Rand (Eds.), *Dynamics, Games and Science II*, Berlin, Heidelberg, pp. 735–752. Springer Berlin Heidelberg.